UNIVERSITY OF STRATHCLYDE
DEPARTMENT OF SHIP AND MARINE TECHNOLOGY
Workshop on Numerical and Physical Simulation of Ship Capsize in Heavy Seas
Ross Priory, Loch Lomond, Glasgow, SCOTLAND
24-25 July 1995

WATER-ON-DECK ACCUMULATION STUDIES BY THE SNAME AD HOC RO-RO SAFETY PANEL

Bruce L. Hutchison[1]

ABSTRACT

A mathematical theory is presented for the accumulation of water on the deck of a damaged RO-RO passenger vessel. Excellent agreement is demonstrated between results obtained from extensive time domain simulations and corresponding results obtained from integrals in the probability domain. Comparison is also made to results obtained during free floating model tests in waves at National Research Council Canada, Institute for Marine Dynamics (IMD). The mathematical theory presented leads to a simple curvilinear relationship between the accumulated depth of water on deck, freeboard and significant wave height. Also briefly addressed are out-flow processes through freeing ports.

1. THE SNAME AD HOC RO-RO SAFETY PANEL

The Society of Naval Architects and Marine Engineers (SNAME) Ad Hoc RO-RO Safety Panel was created in 1994 in response to the capsize and sinking of the *Estonia*. The Ad Hoc Panel is composed of owners and operators, regulators, designers, researchers and academics from both Canada and the United States.

The SNAME Ad Hoc Panel agrees that it is necessary to develop requirements that address the hazard posed by water on the decks of vessels such as fully enclosed RO-RO passenger ferries. The Panel believes that any proposal to address the water-on-deck hazard should be rationally based on:

- The operating environment
- The freeboard at the point of assumed damage
- The means to remove water from the vehicle deck

The SNAME Ad Hoc RO-RO Safety Panel has addressed the problem of water accumulation on deck using time domain simulation and integral methods based on the Gaussian distribution of wave elevations. It is this research by the Panel that is the primary focus of this synoptic paper.

RO-RO Stability Issues Considered by IMO

The goal of the IMO rule making process is to draft new rules that force each vessel to have some combination of stability parameters and subdivision (including subdivision of the RO-RO cargo space) such that the accumulation of an asymptotic average burden of water on deck does not lead to capsize or progressive flooding. The goal in developing new rules is then to:

1. Determine the asymptotic average water-on-deck burden;
2. Establish stability criteria that will lead to survival when a vessel is burdened with the asymptotic average water-on-deck quantity.

The currently proposed IMO rules seek only to apply the SOLAS 90 residual stability criteria to a vessel burdened with water on deck. Whether this is appropriate is an open question, but no serious debate has developed at this time that would lead to the imposition of any other residual stability standard. In the aftermath of the *Herald of Free Enterprise* casualty, research was begun at British Maritime Technology (BMT), Danish Maritime Institute (DMI), Institute for Marine Dynamics (IMD), and the University of Strathclyde. It is hoped that this research may eventually lead to a sound scientific basis for either the endorsement of the SOLAS 90 residual stability criteria for vessels burdened with water on deck, or to the establishment of new residual criteria appropriate to this situation.

In the absence of any serious debate regarding the residual stability standard to be required of vessels burdened with water on deck, the only major remaining topic is the determination of the asymptotic average water-on-deck burden. The SNAME Ad Hoc RO-RO Safety Panel has focused its attention on this remaining topic.

---

[1] Vice President, Ocean Engineering & Analysis, The Glosten Associates, Inc., Seattle, Washington; Chairman, SNAME Ad Hoc RO-RO Safety Panel

2. STATIONARY SHIP MODEL

In consideration of:

1) the research efforts addressing the complete problem at BMT, DMI, IMD, University of Strathclyde, and elsewhere,

2) the ambitious pace set by IMO and the Panel of Experts for development of new rules,

and

3) the manifest preference of IMO and the Panel of Experts for new rules exhibiting the utmost simplicity,

the SNAME Ad Hoc Panel determined to investigate a highly simplified model for the accumulation of water on the deck of a damaged RO-RO vessel. The SNAME Ad Hoc Panel assumed a stationary ship with a flat deck and side damage represented by a rectangular opening of unlimited vertical extent beginning at the deck. The assumed stationarity corresponds to no vessel motion in response to waves (no sinkage, trim or heel), resulting in a fixed elevation, f, of the deck at the point of assumed side damage. The treatment of essential fluid flow processes in the stationary ship model is two-dimensional.

A partial rationale for the stationary ship approach is that, once new rules are implemented, the burden of water on deck is supposed to be limited to a quantity that the vessel can survive without capsize. This argument helps to explain why it may be possible to ignore sinkage, trim and heel. It remains to be established from experiments whether relative motion effects, hydrodynamic interaction between the hull and the waves, or internal dynamics of the accumulated water pool, lead to excessive departures from the expectations based on the stationary ship concept. However, as will be shown later in this synoptic paper, encouraging agreement has been found between predictions based on the stationary ship concept and model test data obtained using a free floating model at IMD.

The Two Phases of the SNAME Panel's Research

In order to appreciate the following presentation of results obtained by the SNAME Ad Hoc Panel it is necessary to explain that its analytical work has proceeded through two phases. The first phase encompasses all work accomplished through 28 February 1995 and culminated in the submission of references 1 and 2 to the IMO Panel of Experts. The second phase comprises that work accomplished since 28 February 1995.

The work accomplished during the first phase of the SNAME Panel's analytical research was grounded on a weir flow equation embodying a velocity superposition principle such that the instantaneous differential flow rate, dQ , at any elevation, is given by:

$$dQ = K\left\{\sqrt{h_{OUT}} - \sqrt{h_{IN}}\right\} dA \qquad (1)$$

where: K is an empirical weir flow coefficient.

h_{IN} is the instantaneous head measured on the inside of the flux plane at any specified elevation above the deck.

h_{OUT} is the instantaneous head measured on the outside of the flux plane at any specified elevation above the deck .

dA is the differential element of flow area in the flux plane at the specified elevation, dA = W dz, where W is the width of the damage opening and dz is a differential element of elevation

During the first phase of the SNAME Ad Hoc Panel's research this velocity superposition expression was applied in those regions (elevations) where water exists on both sides of the flux plane.

In those regions where instantaneously either $h_{IN} = 0$ or $h_{OUT} = 0$, equation 1 is equivalent to the following pressure head weir flow equation which was applied everywhere during the second phase of the SNAME Ad Hoc Panel's analytical research:

$$dQ = K\ \mathrm{sign}(h_{OUT} - h_{IN})\sqrt{|h_{OUT} - h_{IN}|}\ dA \qquad (2)$$

In a later section of this synoptic paper it will be demonstrated that there is only a very small difference in water-on-deck results obtained for the stationary ship using the velocity superposition approach of the early phase of the SNAME research, and the pressure head weir flow equation used more recently.

The motivation for exploring the velocity superposition was, and remains, the ability to separate in-flow and out-flow processes. This is much more conducive to a regulatory strategy wherein a basic water-on-deck burden would be determined based on residual freeboard, f, and significant wave height, H_S. The separation of in-flow and out-flow processes then makes it possible to determine a reduction in the water-on-deck burden in a separate regulatory step based on independent calculations of the actual out-flow potential. This procedure is outlined in reference 2.

Independent Parameters

Given the assumption of a stationary ship, the independent problem parameters are reduced to:

A	area of the deck subject to flooding
f	freeboard at the point of assumed damage
W	the width of the damage opening measured normal to the direction of wave travel
H_S	significant wave height

Objectives

The SNAME Ad Hoc Panel's primary objective was to develop simple mathematical relationships for the following, as functions of the independent parameters:

$\overline{Q}_{IN}$	average in-flow rate onto the flooding deck
$\overline{Q}_{OUT}$	average out-flow rate for water draining off the deck through the assumed damage opening
$\overline{D}$	asymptotic average water depth on deck
$\overline{V}$	asymptotic average water volume on deck, (i.e., $\overline{V} = A\,\overline{D}$)

A secondary but important objective of the SNAME Panel's research was to determine out-flow credit functions for deck drains, freeing ports and active deck pumping systems. The development of these out-flow credits is too extensive for inclusion in the limited format of this paper. The subject of out-flow credits is addressed more completely in reference 2. A few results concerning out-flow credits through freeing ports are presented without supporting documentation in later sections of this synoptic paper.

3. VELOCITY SUPERPOSITION RESULTS

Results were obtained both from time domain simulations and from probability domain integrals during the first phase of the SNAME analytical research. The probability domain integrals were based on the Gaussian distribution of wave elevation in an irregular sea. References 1 and 3 provide greater detail regarding the simulation procedures and the development of the Gaussian integrals. A total of 252 time domain simulations were performed.

Figure 1 shows an example time domain simulation record. After approximately 125 seconds the water depth may be seen to attain an average value about which the time domain depth record oscillates thereafter.

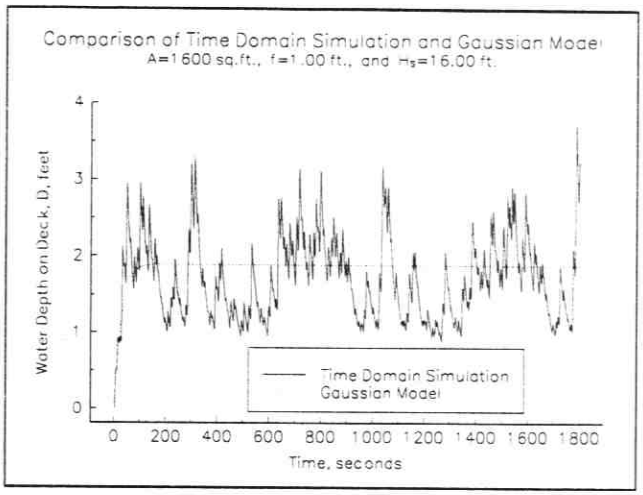

FIGURE 1

Example of Simulated Time Domain Record of Water Depth on Deck

Average In-Flow Rate

When the velocity superposition principle is applied, it is possible to define an average in-flow rate, $\overline{Q}_{IN}$. As may be seen in Figure 2, both the time domain results and the Gaussian model collapse to a single nondimensional functional relationship for $\overline{Q}_{IN}$. The agreement between the Gaussian model and the samples obtained from the time domain simulation is excellent.

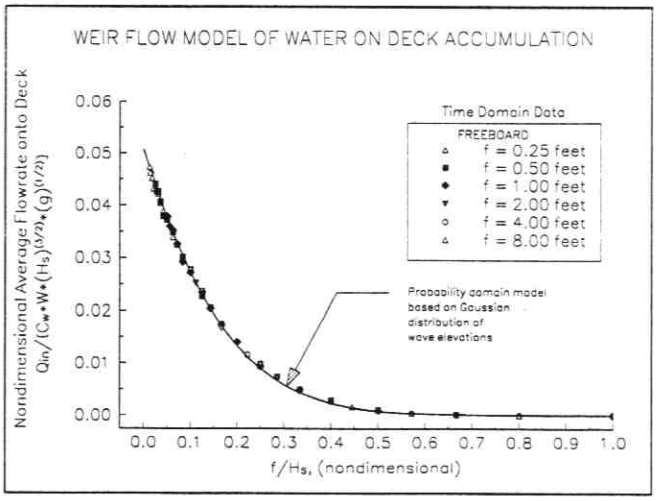

FIGURE 2

Nondimensional In-Flow Rate versus f/H_S

Asymptotic Average Water Depth

Under the assumed velocity superposition principle it is possible to determine the asymptotic average water depth accumulated on deck from the observation that the average in-flow and the average out-flow are equal when the asymptotic average water depth is achieved. Based on this observation, the following equation for the asymptotic average water depth was obtained:

$$W\,C_W\left(\tfrac{2}{3}\right)\sqrt{2\,g}\,\overline{D}^{3/2} = \overline{Q}_{OUT} = \overline{Q}_{IN} \qquad (3)$$

which has as a solution:

$$\overline{D} = \left[\frac{\overline{Q}_{IN}}{W\,C_W\left(\tfrac{2}{3}\right)\sqrt{2\,g}}\right]^{2/3} \qquad (4)$$

Figure 3 presents, in nondimensional form, a comparison between the asymptotic average water depth on deck determined from the Gaussian model, with the sample average values obtained from the time domain simulations. As may be seen in Figure 3 both the time domain results and the Gaussian model collapse to a single nondimensional functional relationship. The agreement between the Gaussian model and the samples obtained from the time domain simulation is excellent.

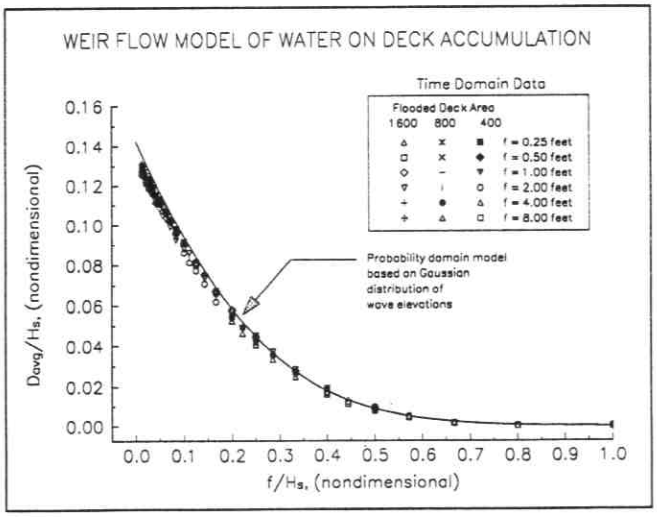

FIGURE 3

Nondimensional Asymptotic Average Water Depth on Deck versus f/H_S

Expected Build-Up Time

As detailed in references 1 and 3, it is possible to derive a closed form expression for the expected value of the water depth as a function of time, in terms of the flooded deck area, A, the width of the damage opening, W, and the average in-flow rate, $\overline{Q}_{IN}$. Since $\overline{Q}_{IN}$ is a function of residual freeboard, f, significant wave height, H_S, and damage width, W, the expected water depth as a function of time depends on A, W, f and H_S.

The dotted line shown in Figures 1 and 4 shows the expected build-up process for water on deck (labeled Gaussian model). As illustrated by Figures 1 and 4 the agreement is excellent between the expected trend and the mean trend of the simulated time domain data.

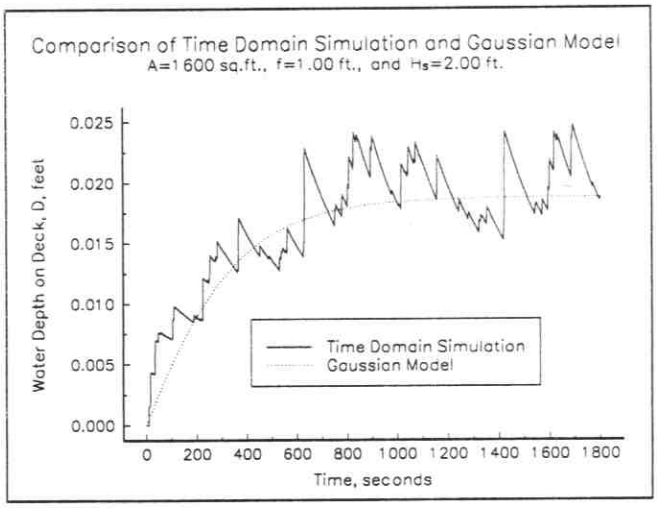

FIGURE 4

Example of Simulated Time Domain Record of Water Depth on Deck, Showing Comparison With the Expected Build-Up Model

Figures 5 and 6 compare the expected (i.e., average) time required to build up to 99% of the asymptotic average water depth with the build-up time required for the first passage above the asymptotic average water depth, as determined from the sample time domain record. Figure 5 is for a flooded deck area of 1,600 square feet while Figure 6 is for a flooded deck area of 400 square feet. The damage width is constant for all cases at W = 10 feet.

The flooded deck area in Figure 5 is four times that in Figure 6 and consequently the build-up time is longer for the cases portrayed in Figure 5 than for the cases in Figure 6.

The build-up time may be seen to be strongly dependent on the value of the asymptotic average water depth on deck. Excepting those cases where the asymptotic average water depth on deck is quite small, the build-up time is quite short. The importance of this

finding is that all the most hazardous cases are achieved with great rapidity; it is only the (most likely) inconsequential cases, where only small average water depths are achieved, that build up slowly.

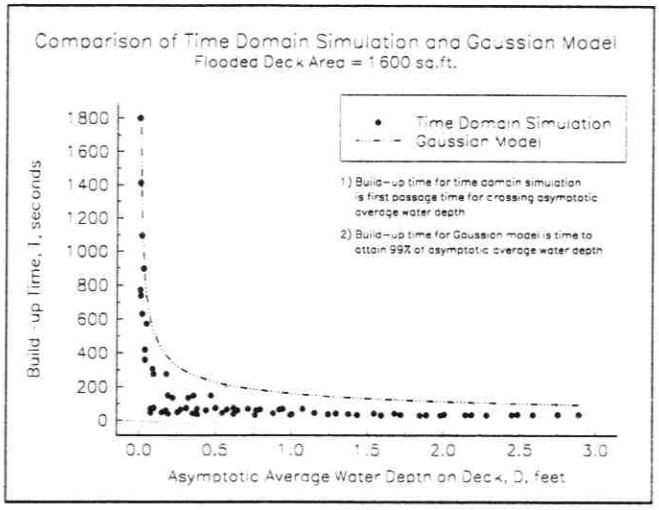

FIGURE 5

Comparison of Build-Up Times Between Time Domain Simulation and Expected Build-Up Model (Labeled Gaussian Model)

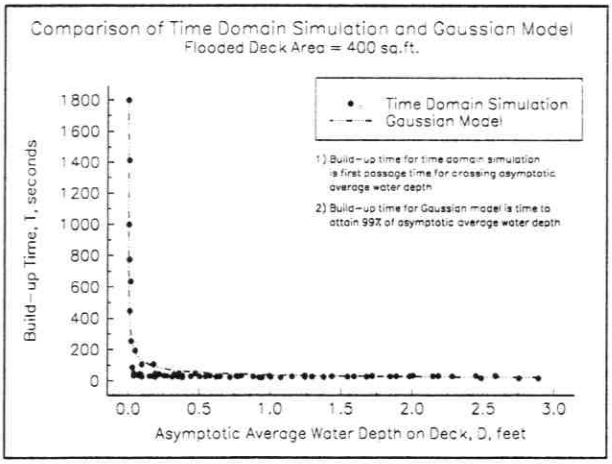

FIGURE 6

Comparison of Build-Up Times Between Time Domain Simulation and Expected Build-Up Model (Labeled Gaussian Model)

Probability Density and Cumulative Probability Distributions

Certain results regarding the stochastic water-on-deck process can be obtained only in the time domain.

Among results that can be obtained from the time domain are sample values for the probability density and cumulative probability distributions for the water depth on deck. Examples of these are shown in Figures 7 and 8.

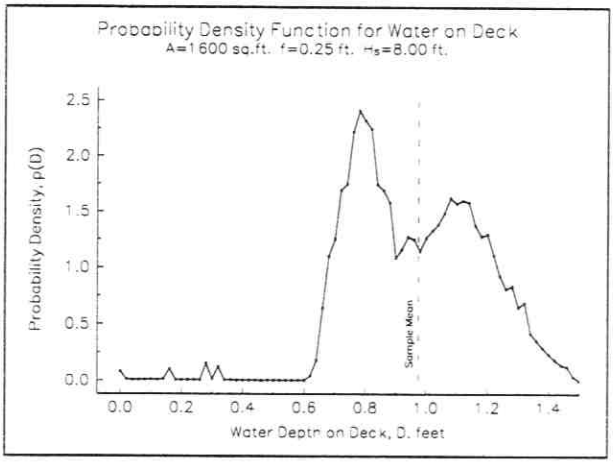

FIGURE 7

Example, Sample Probability Density Function for Water Depth on Deck

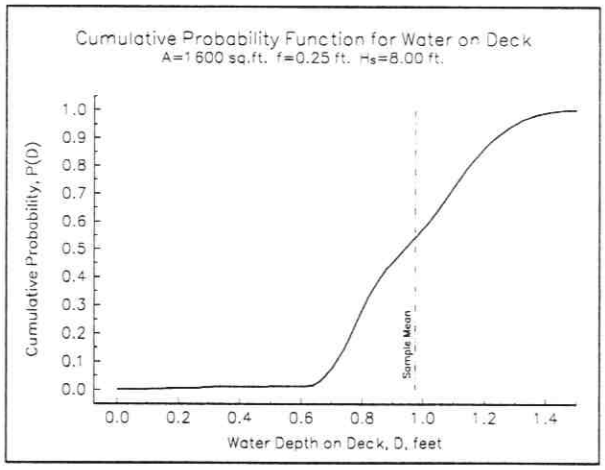

FIGURE 8

Example, Sample Cumulative Probability Distribution of Water Depth on Deck

One of the interesting features is the bi-modal character of the probability density distribution shown in Figure 7. This bi-modal character was observed in many, though certainly not all, of the cases simulated.

Persistence

Another interesting probability result that may be obtained from the time domain simulations is sample values for the persistence of the water depth process. The persistence measures the average duration of the stochastic water depth process above (or below) any specified threshold value. Figure 9 depicts an example of persistence functions sampled in the time domain.

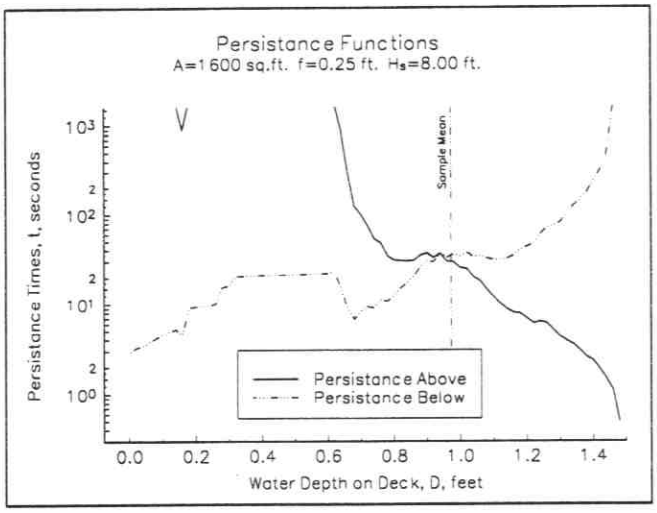

FIGURE 9

Example, Sample Persistence Functions for Water Depth on Deck

Figure 9 indicates that the water depth in this example case persists at or above the asymptotic average water level (sample mean) for an average duration of about 17.5 seconds, and that it persists below that average level for a period of time which averages approximately 20 seconds. The average recurrence interval for process upcrossings of the asymptotic average water depth is the sum of the persistences above and below that threshold, or approximately 37.5 seconds.

The water level in this example case persists at or above a 1.2 foot depth for approximately 7.0 seconds and below this level for approximately 45 seconds.

A study of the dependency trends of persistence with respect to the independent process parameters such as flooded deck area, freeboard, significant wave height and the width of the assumed damage opening, has not been completed at this time.

4. OUTFLOW THROUGH FREEING PORTS

Extensive results were obtained for freeing ports and deck drains (scuppers) during the first phase of the SNAME analytical research using the velocity superposition assumption. These results have been reported in reference 2. Within the confines of this restricted format it is possible to present only a sample of the results obtained for freeing ports.

Basic Approach to Out-Flow Through Freeing Ports

The basic approach to determining the water depth on deck when there is additional outflow through freeing ports is rooted in the observation that, as expressed by equation 3, the asymptotic average water depth is associated with a condition where the average in-flow process balances the average (total) out-flow process. However, where freeing ports, deck drains or other outflow devices in addition to the assumed damage opening are present, the average out-flow rate, $\overline{Q}_{OUT}$, must represent all out-flow processes (i.e., out-flow through the assumed damage opening plus out-flow through freeing ports, etc.).

To be considered effective, freeing ports must be provided with a in-flow excluder device such as a counter-balanced flap that will prevent any significant flow through the freeing port onto the deck, but which will permit flow overboard, off the deck.

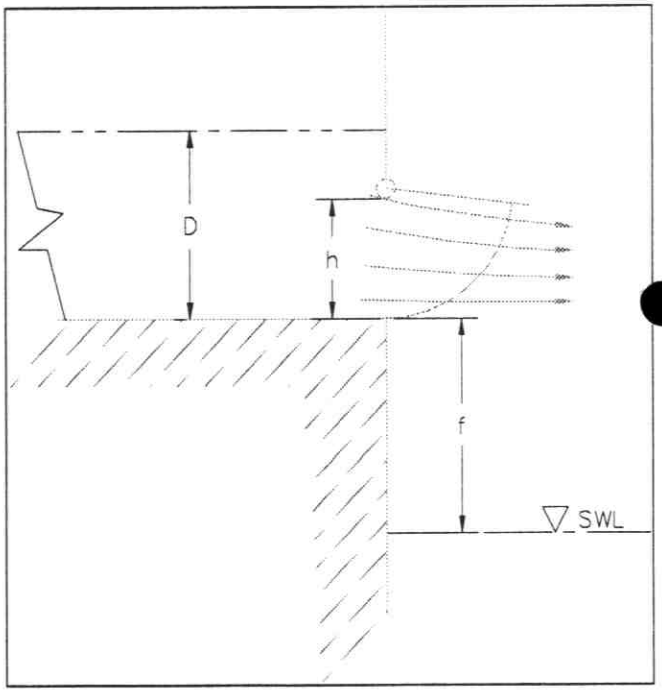

FIGURE 10

Definition Sketch for Freeing Ports

Charts from which the average out-flow of freeing ports may be determined as a function of the depth of water on deck were developed and reported in references 2 and 3. Figure 11 is an example of such an out-flow chart, where:

C_{FP} is a flow discharge coefficient for the freeing port corresponding to the orifice coefficient of basic fluid mechanics. Typical values of C_{FP} are thought to lie between 0.5 and 0.6, with 0.5 being the conservative choice.

W is the (aggregate) width of freeing ports serving the flooded deck area and having the same parameters (i.e., freeing port height, significant wave height).

h is the height of the freeing port opening.

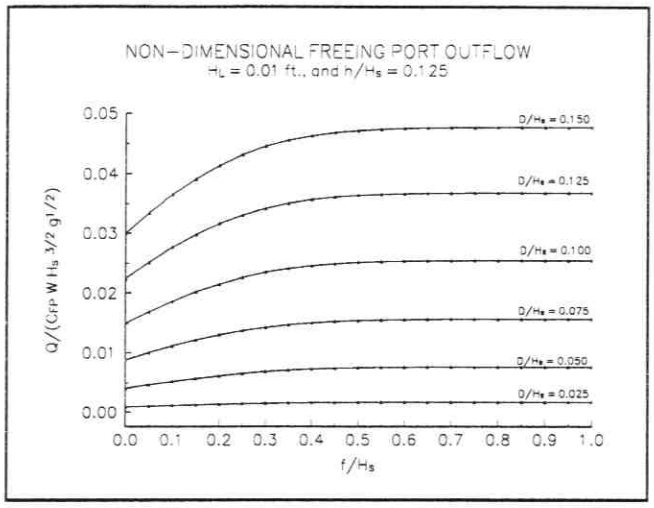

FIGURE 11

Average Outflow Through Freeing Port(s)
With Head Loss of $H_L/H_S = 0.01$ and Freeing Port Height
$h/H_S = 0.125$

Eight charts were developed and reported in references 2 and 3, one each with nondimensional freeing port height: $h/H_S = 0.025$, 0.050, 0.075, 0.100, 0.125, 0.150, 0.175, and 0.200. The assumed nondimensional head loss for all of the charts is constant, with $H_L/H_S = 0.01$, where H_L is the head loss. Actual freeing port flows with values of nondimensional freeing port height between $0.025 \le h/H_S \le 0.200$ can be determined by linear interpolation among the charts provided.

Each of the charts given in references 2 and 3 shows curves of constant water depth on deck nondimensionalized by the significant wave height with values of:

$D/H_S = 0.025$, 0.050, 0.075, 0.100, 0.125 and 0.150

which span the range of expected values. The outflow for $D/H_S = 0.00$ is zero. Outflow at intermediate values of D/H_S may be determined by interpolation.

Freeing Port Performance in the Time Domain

During the first phase of the SNAME Ad Hoc Panel's analytical studies a limited number of time domain simulations were performed that included freeing ports. Figure 12 compares the water-on-deck time history, with and without freeing ports, for an example case with a freeboard of 0.25 feet (0.076 m), a significant wave height of 8.0 feet (2.44 m) and a flooded deck area of 1,600 sq.ft. (149 m^2). The freeing port modeled in this time domain case had an aggregate width of 20 feet and a height of 1.0 foot. The width of the assumed damage was 10 feet. Thus the ratio of the freeing port width to the assumed damage width was, $W_{FP}/W = 2.0$, and the ratio of the freeing port height to the significant wave height was $h/H_S = 0.125$.

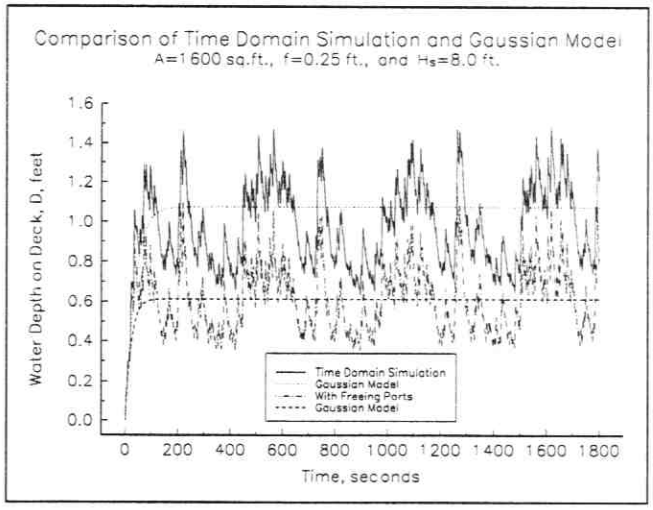

FIGURE 12

Time History of Water Depth on Deck
Comparison Case With and Without Freeing Ports

Figure 13 shows the sample probability density functions for the same comparison case, with and without freeing ports.

It may be seen in both Figures 12 and 13 that the general character of the water-on-deck process is

preserved, but that it occurs about a lower mean value when freeing ports are provided. For the example shown the ratio of the average water depth with freeing ports to that without freeing ports is about 0.57.

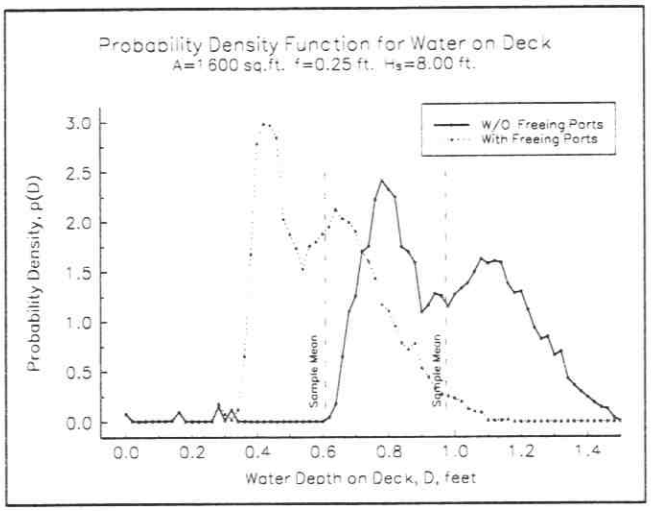

FIGURE 13

Sample Probability Density Functions for Water Depth on Deck Comparison Case with and Without Freeing, with Head Loss of $H_L/H_S = 0.01$ and Freeing Port Height $h/H_S = 0.200$

References 2 and 3 contain discussion and examples of how out-flow credits could be applied in a simple and practical procedure suitable for inclusion in a regulatory framework.

General Effectiveness of Freeing Ports

The effectiveness of freeing ports in reducing the depth of water on deck is strongly dependent on the ratio of the aggregate width of freeing port to the width of assumed damage, W_{FP}/W. Figure 14 plots 1330 cases produced by systematically varying the following parameters:

- f freeboard
- H_S significant wave height
- h height of freeing port opening

and the ratio of aggregate freeing port width to width of assumed damage, W_{FP}/W.

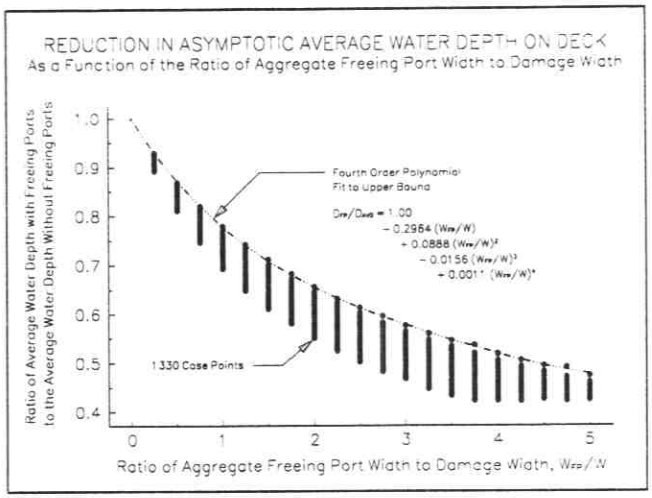

FIGURE 14

General Effectiveness of Freeing Ports as a Function of the Ratio W_{FP}/W Showing Fourth-Order Polynomial Fit to Upper Bound

Also shown in Figure 14 is a fourth-order polynomial fit to the upper bound of the computed case points. The fourth order polynomial has the equation:

$$\frac{D'_{FP}}{\overline{D}} = 1.0 - 0.2964\left(\frac{W_{FP}}{W}\right) + 0.0888\left(\frac{W_{FP}}{W}\right)^2 - 0.0156\left(\frac{W_{FP}}{W}\right)^3 + 0.0011\left(\frac{W_{FP}}{W}\right)^4 \quad (5)$$

where: D'_{FP} is the asymptotic average water depth with outflow through both the damage opening and freeing ports

$\overline{D}$ is the asymptotic average water depth with outflow only through the damage opening

W_{FP} is the aggregate width of the freeing ports serving the flooded deck area

W is the damage width

Other Outflow Issues

Reference 2 may be consulted for details of the development of the freeing port outflow and also for similar development regarding outflow through deck drains (scuppers). Other issues discussed in reference 2 include the effect of casings on outflow processes, the attenuation of the significant wave height on the lee side of the vessel, and the effect of freeing port height on the general effectiveness of freeing ports.

It should be noted that in the first phase of the SNAME research, freeing ports and deck drains (scuppers) were shown to be complementary. Freeing ports are most effective in removing large volumes of water from the deck, but lose their effectiveness when the water depth on deck becomes small. Deck drains are not particularly effective in removing large volumes of water, but, because of the suction head in the deck drain tailpipe, deck drains are more effective than freeing ports in removing small residual depths of water from the deck.

5. PRESSURE HEAD FORMULATION OF WEIR FLOW EQUATION RESULTS

Subsequent to the 28 February 1995 submission of references 1 and 2 to the IMO Panel of Experts, and prompted by correspondence with Dr. Vassalos of the University of Strathclyde, the SNAME Ad Hoc Panel investigated the application of the pressure head weir flow, equation 2, throughout. On theoretical grounds the pressure head form of the weir flow equation is regarded as more correct and accurate than the velocity superposition form applied during the first phase of the SNAME analytical studies, but the disadvantage is the loss of separation between in-flow and out-flow processes.

As will be shown in the following development, the method of Gaussian integral equations may be also applied when using the pressure head formulation of the weir flow equation and the final results differ by only a small amount from those obtained using the velocity superposition method. Thus, for the purposes of regulation and rule making it may suffice to adopt the velocity superposition method and gain the advantages associated with the separation of in-flow and out-flow processes.

It should also be noted that, for the purposes of scientific investigation and engineering, but probably not for the purposes of regulation and rule making, the method of Gaussian integral equations may be applied to cases based entirely on the pressure head formulation of the weir flow equation, and including additional outflow devices such as flow biased freeing ports and deck drains.

The fundamental idea behind the analysis that follows is that the average net volume flux is zero once equilibrium has been established between the in-flow and out-flow processes.

Figure 15 is similar to Figure 3. Figure 15 shows two curvilinear lines, one marked "Weir Flow Model, Based on Velocity Superposition" and the other marked "Weir Flow Model, Based on Pressure Head." Also shown is a straight line approximation suggested by the SNAME Ad Hoc RO-RO Safety Panel to the IMO Panel of Experts, and data from the IMD model tests (which will be discussed in a subsequent section of this synoptic paper).

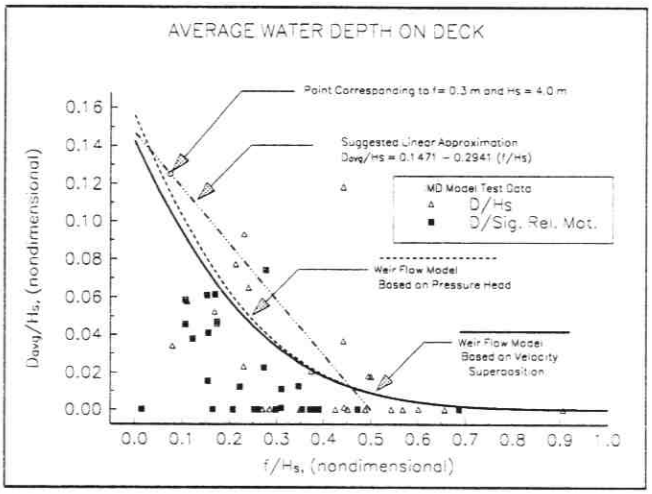

FIGURE 15

Comparison of Asymptotic Average Water Depth on Deck As Estimated by Pressure Head and Velocity Superposition Forms of the Weir Flow Equation

The curve marked 'Weir Flow Model, Based on Pressure Head' was obtained using the Gaussian integral approach by solving the following equation for unknown asymptotic average water depth D:

$$\overline{Q}_{NET} = 0 = \int_{f+D}^{\infty} N(0,\sigma,\eta)\left\{K\,W\left(\frac{2}{3}\right)(\eta - f - D)\sqrt{(\eta - f - D)}\right\}\,d\eta$$

$$+ \int_{f+D}^{\infty} N(0,\sigma,\eta)\left\{K\,W\,D\sqrt{(\eta - f - D)}\right\}\,d\eta$$

$$+ \int_{f}^{f+D} N(0,\sigma,\eta)\left\{K\,W\left(\frac{2}{3}\right)(f + D - \eta)\sqrt{(f + D - \eta)}\right\}\,d\eta$$

$$+ \int_{f}^{f+D} N(0,\sigma,\eta)\left\{K\,W\,(\eta - f)\sqrt{(f + D - \eta)}\right\}\,d\eta$$

$$+ \int_{-\infty}^{f} N(0,\sigma,\eta)\left\{K\,W\left(\frac{2}{3}\right)D\sqrt{D}\right\}\,d\eta \qquad (6)$$

where:

K	is a dimensional flooding coefficient
W	is the width of the damage opening
f	is the freeboard
H_S	is the significant wave height
η	is the wave elevation
σ	is the standard deviation of the wave elevation process, $\sigma = H_S / 4$

and

$N(0,\sigma,\eta)$	is the Gaussian (normal) probability density function with zero mean and standard deviation, σ

$$N(0,\sigma,\eta) = \frac{e^{-\left\{\eta^2/2\sigma^2\right\}}}{\sigma\sqrt{2\pi}}$$

Note that the factor K W is a common factor which may factored out of equation 6.

There are five integrals in this equation. The situations that give rise to these integrals is depicted in Figures 16 through 18, which follow.

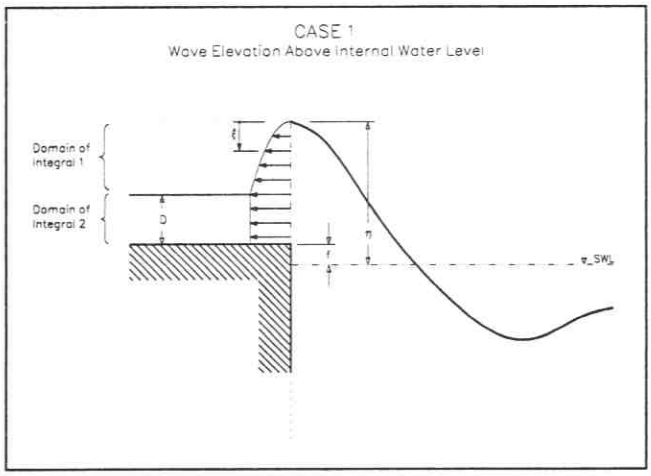

FIGURE 16

Figure 16 depicts those cases where the wave elevation is above the internal water level. This situation gives rise to two integrals. Integral 1 corresponds to the flow into the vessel from the wave surface down to the internal water level. In this region the fluid velocity is $v_1 = K\sqrt{\xi}$ according to both the pressure head and velocity superposition approaches, and the volume flow rate is $Q_1 = K\,W\left(\frac{2}{3}\right)(\eta - f - D)\sqrt{(\eta - f - D)}$. Integral 2 corresponds to the flow into the vessel which takes place in the vertical region from the surface of the internal water level down to the deck. According to the pressure head equations the fluid velocity in this region takes on a constant value given by $v_2 = K\sqrt{(\eta - f - D)}$. And, according to the pressure head approach, the volume flow rate is $Q_2 = K\,W\,D\sqrt{(\eta - f - D)}$.

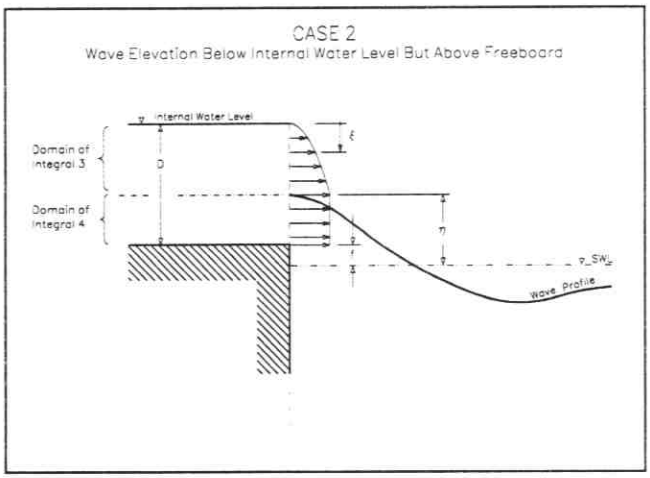

FIGURE 17

Figure 17 depicts those cases where the wave elevation is below the internal water level but above the freeboard elevation. This situation gives rise to two integrals. Integral 3 corresponds to the flow out of the vessel from the internal water depth that lies above the wave elevation, down to the wave elevation. In this region the fluid velocity is $v_3 = K\sqrt{\xi}$ according to both the pressure head and velocity superposition approaches, and the volume flow rate is $Q_3 = K\,W\left(\frac{2}{3}\right)(f + D - \eta)\sqrt{(f + D - \eta)}$. Integral 4 corresponds to the flow out of the vessel which takes place in the vertical region from the wave surface down to the deck. According to the pressure head equations the fluid velocity in this region takes on a constant value given by $v_4 = K\sqrt{(f + D - \eta)}$. And, according to the pressure head approach the volume flow rate is $Q_4 = K\,W(\eta - f)\sqrt{(f + D - \eta)}$.

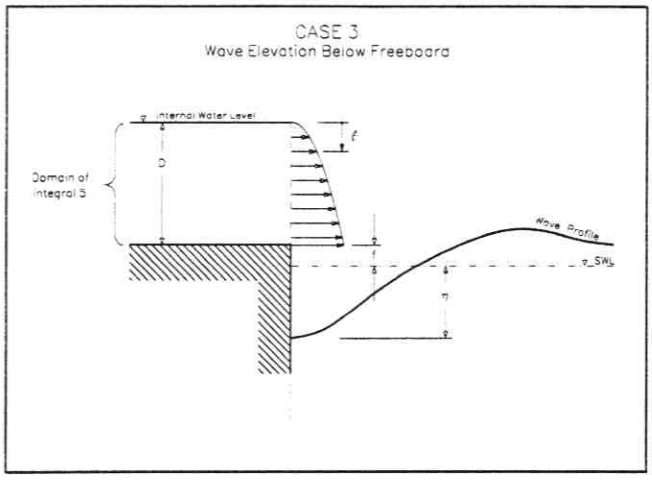

FIGURE 18

Figure 18 depicts those cases where the wave elevation is below the freeboard elevation. This situation gives rise to one integral. Integral 5 corresponds to the flow out of the vessel from the internal water depth down to the deck. In this region the fluid velocity is $v_5 = K\sqrt{\xi}$ according to both the pressure head and velocity superposition approaches, and the volume flow rate is $Q_5 = K\,W\left(\frac{2}{3}\right)D\sqrt{D}$.

The equation for D has been solved using a numerical root finding procedure. The result is the curve shown in Figure 15 labeled "Weir Flow Model, Based on Pressure Head" and graphed using a short dashed line. As shown in Figure 15, the pressure head equations lead to a slightly greater predicted depth of water on deck at low freeboard values when compared with the corresponding results obtained from the velocity superposition equations, but the difference is not large. At values of f/H_S greater than 0.45 the difference is negligible. The pressure head equations approach more closely the point of interest to certain Nordic parties, corresponding to 0.5 m of water depth in 4.0 m significant waves for a vessel with 0.3 m freeboard.

Overall, there is excellent agreement between the *pressure head* and *velocity superposition* weir flow models. The advantage which the SNAME Ad Hoc Panel finds with the velocity superposition method is the ability to de-couple the in-flow and out-flow processes, which greatly facilitates the process of evaluating out-flow credits for freeing ports and deck drains, as was done in references 2 and 3.

One final result obtained based on the pressure head formulation of the weir flow equation using the method of Gaussian integral equations is presented in Figure 19 without development.

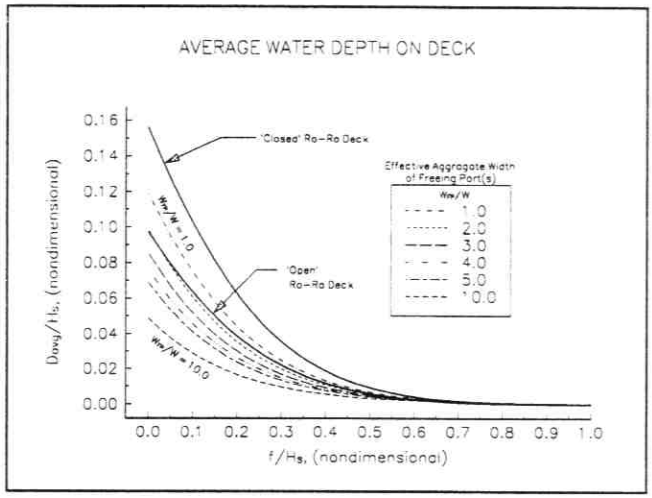

FIGURE 19

Freeing Port Performance Obtained Based on Pressure Head Formulation of Weir Flow Equations Using the Method of Gaussian Integral Equations

The curve in Figure 19 labeled " 'Closed' Ro-Ro Deck" corresponds to the curve in Figure 18 labeled "Weir Flow Model, Based on Pressure Head." Six curves are shown in Figure 19 for freeing ports with a height ratio of $h/H_S = 0.125$, corresponding to freeing port aggregate width ratios, W_{FP}/W, of: 1.0, 2.0, 3.0, 4.0, 5.0 and 10.0. Also shown is a curve labeled " 'Open' Ro-Ro Deck," which was obtained for the stationary ship by permitting out-flow both through the damage opening and through a permanent opening of width, W, on the leeward side of the vessel (and assuming no waves on the leeward side).

Figure 19 indicates that, for the case of the stationary ship, flow biased freeing ports ($h/H_S = 0.125$) with an aggregate width twice the width of damage at the deck edge are as effective as a completely open deck. Flow biased freeing ports with an aggregate width four times the width of damage will result in a reduction to approximately 50% of that obtained without freeing ports.

6. COMPARISON WITH PHYSICAL MODEL TEST RESULTS

The findings of this analytical study have been compared with data measured in physical model tests at National Research Council Canada, Institute of Marine Dynamics (IMD) (references 4 & 5). Those physical model tests have also been presented in SLF39/INF.16.

The model tests at IMD were of a prismatic ship floating in waves with six degrees-of-freedom. The tests therefore do not correspond precisely with the assumptions inherent in the study of a stationary ship. Of the many cases studied in the IMD experiment program, only those cases that did not capsize are a source for data regarding the asymptotic average water volume and depth.

For the stationary assumptions in the simulation, the relative motion is the same as the wave height. The experimental points are plotted in two ways in Figure 15. The first method of plotting the points (corresponding to the open triangle symbols) made use of the significant wave height to normalize both freeboard and average water depth on deck. In the second method of plotting the experimental points (corresponding to the solid square symbols) the freeboard and average water depth are normalized by the significant double amplitude of relative motion (between the deck edge and the local wave surface) measured at the point of damage, instead of the significant wave height. There is slightly less scatter of the experiment results normalized by relative motion and the theoretical line is more conservative than the observed data when presented on the basis of relative motion.

There are few experimental points shown in Figure 15 at low values of f/H_S, and those few do not approach the theoretical curve. The theoretical curve is for a stationary ship that does not sink, trim, heel or capsize in response to the water burden on deck. The experimental points are for a free floating model which will in fact sink, trim, heel, and sometimes capsize. However, the experimental points in Figure 15 were only obtained from those cases where the model did not capsize and an asymptotic average water accumulation could be determined. Most experimental cases with a free floating ship and very small freeboard (i.e., small f/H_S) ended in capsize, and therefore no asymptotic average water accumulation could be determined. The measured data confirm the predictions that above a certain ratio of freeboard to wave height there is very little water on the deck.

There is an interesting observation that even at relatively low values of f/H_S there are also some cases when there are very low volumes of water on the deck. Although the instrumentation in the model was not designed to measure very low values of water, video records of the experiments confirmed that the volumes of water on the deck in these cases were negligible.

From the video tapes, it was seen that below a critical value of wave height, a lot of the water was coming onto the deck through the damage in the deck and not through the side. In these cases it was very easy for the water to drain back out through the hole in the deck, without flooding it. The other factor that has to be considered is the relationship between relative motion and roll angle. The flow of water onto the deck did not become significant until the root-mean-square roll angle was greater than approximately 2 degrees. In these cases the majority of the relative motion was coming from heave. The water remained relatively static and easily drained off the deck. For higher roll angles, a wave system built up on the deck which affected the drainage rates. None of these factors are included in the simulations, since the only route for the flood water was through the damage in the side.

7. DEPENDENCIES INDICATED BY MATHEMATICAL MODEL

The dependence of the main dependent variables examined in this paper on the independent parameters, is summarized in the following table.

TABLE 1

Dependence of Dependent Variables on Independent Parameters

Dependent Variables		Independent Parameters				
		f	H_S	W	A	C_W
Average In-Flow Rate	$\overline{Q}_{IN}$	YES	YES	YES	NO	YES
Average Out-Flow Rate	$\overline{Q}_{OUT}$	YES	YES	YES	NO	YES
Asymptotic Average Water Depth	$\overline{D}$	YES	YES	NO	NO	NO
Average Build-Up Time	t	YES	YES	YES	YES	YES

The most important result is that, under the assumptions of this study, the asymptotic average water depth is independent of the width of the assumed damage opening, the flooded deck area, and the weir flow coefficient. The only dependencies for the asymptotic average water depth of the stationary ship are freeboard and significant wave height.

8. FUTURE RESEARCH

The SNAME Ad Hoc RO-RO Safety Panel is cooperating with other U.S. and Canadian organizations to guide additional research using physical model and analytical methods. The intention is for the research to focus on problems of particular interest to North American RO-RO passenger vessels, and not to duplicate European research efforts. Current plans are for:

1) Additional model tests to study the effectiveness of freeing ports on different deck arrangements found on North American ferries, including bulwarks, decks enclosed at the bow and decks enclosed at the bow and stern. These tests will be carried out at the Institute for Marine Dynamics for Transport Canada.
2) Additional studies of the so-called "bow scooping" process with models representative of ferries operating in Canada and the U.S. This work will be carried out at B.C. Research.
3) Analytical research to extend the earlier SNAME Ad Hoc RO-RO Safety Panel studies to include: a) vessel heave and roll motion; b) water sloshing on the RO-RO deck; and c) the bow scooping process associated with open bows and forward speed in waves. This work will be performed by The Glosten Associates.
4) Physical tests at full scale of the hydraulic effectiveness of various freeing port designs. These tests will most likely be performed at B.C. Research.

This work will address important aspects of the proposed amendments to the SOLAS regulations concerning relationships between residual freeboard, wave height and area of freeing ports for ships which are not fully enclosed.

It is hoped that the first three elements of the continued research program outlined above can be completed before the SOLAS Convention scheduled to take place in November 1995.

Funding and guidance for this continued research program is being provided by the Canadian and U.S. Coast Guards, the Society of Naval Architects and Marine Engineers, U.S. and Canadian ferry owner/operators and the Canadian Transport Development Centre.

9. ACKNOWLEDGMENTS

The SNAME Ad Hoc RO-RO Safety Panel wishes to acknowledge joint industry financial assistance supporting this research effort from Washington State Ferries, the Alaska Marine Highway System, and The Glosten Associates, Inc.

The mathematical theories that were developed were compared with model test data for damaged ships freely floating in waves, which had previously been performed at National Research Council Canada, Institute for Marine Dynamics, under joint sponsorship of the Transportation Development Centre and Canadian Coast Guard, Ship Safety Branch and the Institute for Marine Dynamics.

This synoptic technical paper is substantially based on a paper originally presented at Cybernautics 95, SNAME California Joint Sections Meeting, held aboard the *Queen Mary* at Long Beach, California, 21-22 April 1995 (reference 3). Co-authors David Molyneux of IMD and Patrick Little of the U.S. Coast Guard contributed to the original source paper.

REFERENCES

1. "Water Accumulation on the Deck of a Stationary Ship," Annex A to the second position paper submitted 28 February 1995 to the IMO Panel of Experts by the SNAME Ad Hoc RO-RO Safety Panel
2. "Freeing Port Effectiveness of Water on Deck," Annex B to the second position paper submitted 28 February 1995 to the IMO Panel of Experts by the SNAME Ad Hoc RO-RO Safety Panel
3. Hutchison, B.L., Molyneux, D. and Little, P., "Time Domain Simulation and Probability Domain Integrals for Water on Deck Accumulation," Cybernautics 95, SNAME California Joint Sections Meeting, held aboard the *Queen Mary* at Long Beach, California, 21-22 April 1995
4. Pawlowski, J.S., Molyneux, D., and Cumming, D. "Analysis of Experience on RO-RO Damage Stability," IMD TR-1994-27, Oct. 1994 (protected)
5. Molyneux, D., "Estimates of Steady Water Depths on the Deck of a Damaged RO-RO Ferry Model," IMD TR-1995-26 (in preparation)

PRELIMINARY STUDY TOWARDS A CAPSIZING SIMULATOR

Kazuhiko Hasegawa, Masami Hamamoto
Department of Naval Architecture and Ocean Engineering,
Faculty of Engineering,
Osaka University,
2-1, Yamada-oka, Suita, Osaka, 565 Japan

Hiroyuki Kotani[1]
Matsushita Electric Company,
1006, Kadoma, Osaka, 571 Japan

ABSTRACT

A prototype of capsizing simulator is introduced as well as some historical review of computer graphics usage on the research of ship capsizing. Connecting two EWS/GWS's and a PC through LAN or serial communication line, real-time calculation and graphical presentation of ship motion of 6 degrees-of-freedom is realized. Displaying the graphical output on a video projector through a scan converter, a simple but powerful capsizing simulator is completed. As an example of the application, the verification of an operational guidance to avoid capsizing is shown.

INTRODUCTION

The new technology, especially that of computer hardware and software has brought us various benefits in almost all fields. In our laboratory, where we are dealing with various problems concerning ship manoeuvrability, motions and control, we had to and do always face to the front end in both theoretical and experimental approaches. In this paper, we will introduce an example from our experiences. It is on capsizing, one of the oldest, but at the same time the hottest topics in naval architecture.

[1]Graduate student, Osaka University at the time of the research

TIME-DOMAIN SIMULATION OF CAPSIZING IN WAVES

Capsizing in waves is a non-linear phenomenon. It is very difficult to treat it theoretically. Well-known strip theory itself is derived under the assumption that the wave height is much smaller than the wavelength, so it is not applicable to this problem. Hamamoto and others [1-11] have engaged in this problem for a long time and developed the equations of the motion applicable to severe motion of six degrees-of-freedom (Hamamoto et al. [9]). Time-domain simulation as well as free-running experiments thus become important except some simplified stability analysis (e.g. Hamamoto et al. [11]).

An example of such a time-domain simulation as well as the result of the corresponding experiment of a container ship, whose particulars and body plan are in Table 1 and Fig. 1 respectively, is shown in Fig. 2 (Hamamoto et al. [3]). It is a kind of way to explain the phenomenon. After a careful looking into the figure, one may understand the motion and find the model ship has capsized around 7 seconds after the start.

Table 1
Principal particulars of the ship and its model

	Ship	Model
L (m)	115.	2.5
B (m)	19.	.413
d (m)	6.4	.139
V (m^3)	9859.	.101
S (m^2)	2945.	1.345
C_b	.705	.705
C_w	.97	.97
B/d	2.97	2.97
L/B	6.05	6.05
		1/46

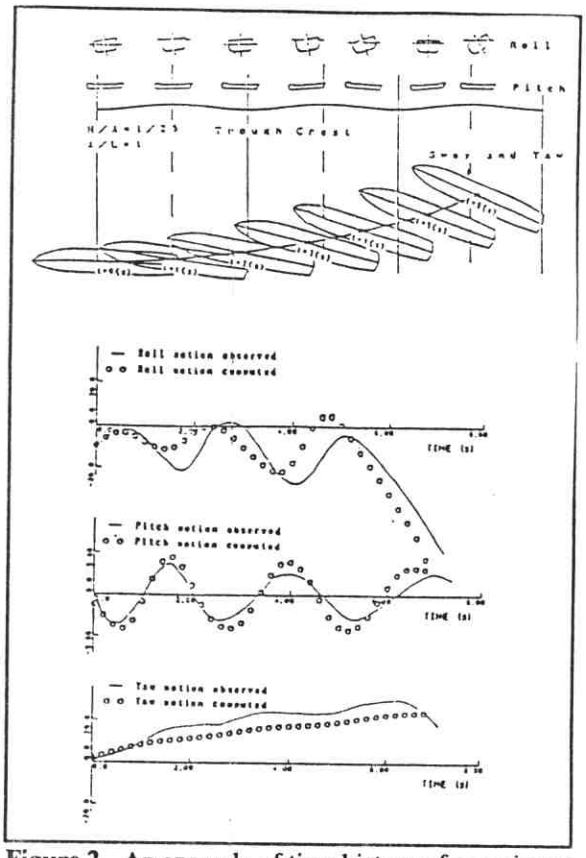

Figure 2. An example of time history of experiment and corresponding simulation

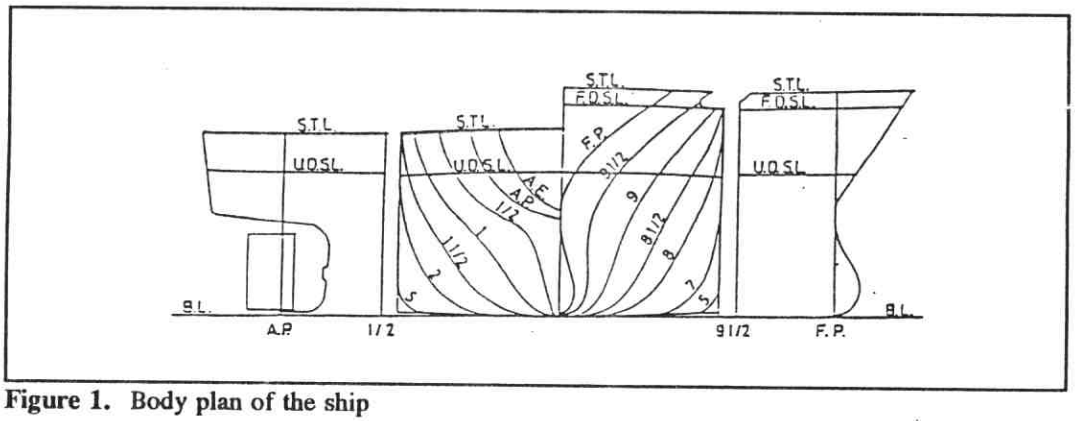

Figure 1. Body plan of the ship

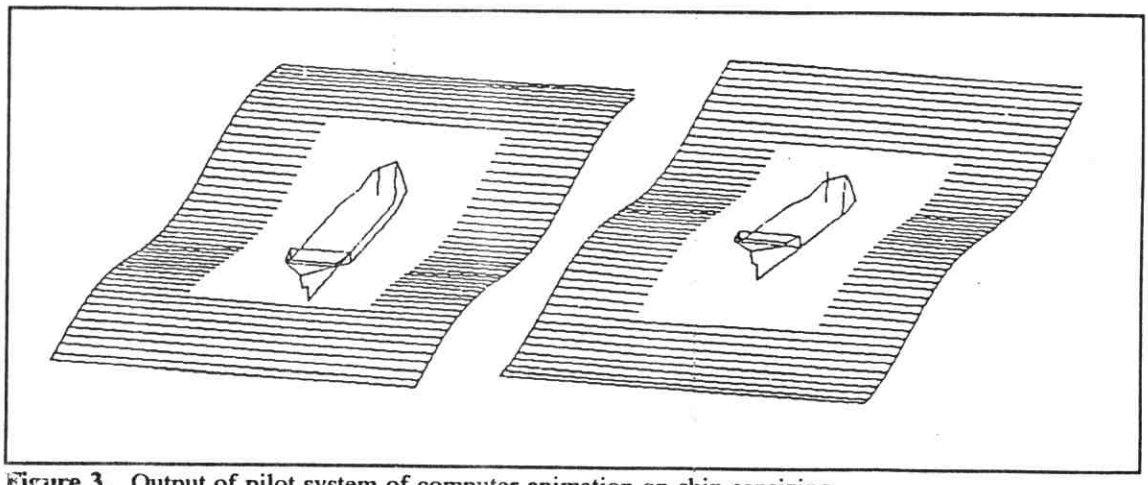

Figure 3. Output of pilot system of computer animation on ship capsizing

COMPUTER ANIMATION FOR CAPSIZING MOTION

The advanced technology in computer graphics will make it more intuitive, when it is prepared in animated motion. The first author has tried to apply it from the early stage of the research. Fig. 3 is such an example done in 1988. At that time wire-frame model using a mini-computer (HP1000) was only available in their laboratory and it took about 5 seconds to make one picture. Besides, wave surface around the ship was omitted to avoid time-consuming calculation for hidden lines. However, it was really impressive to see the dynamic movement of the ship up to capsizing.

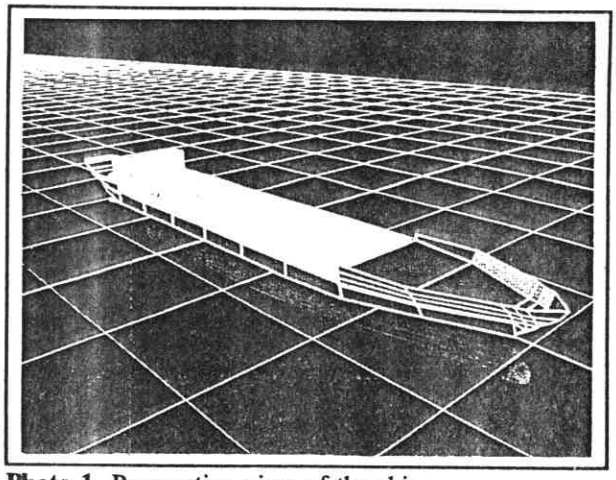

Photo 1. Perspective view of the ship

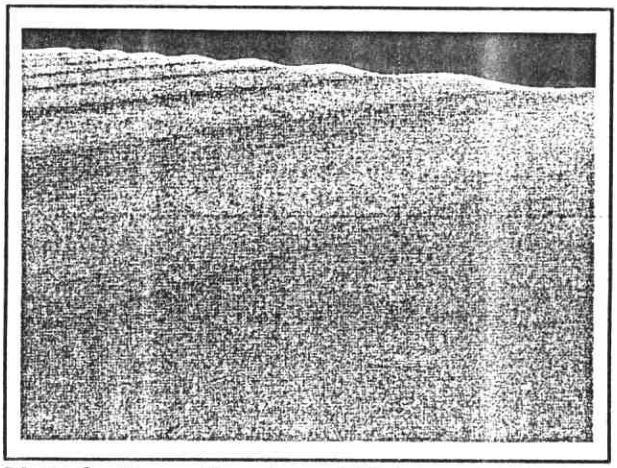

Photo 2. Perspective view of 2D wave

The pilot system thus developed has encouraged us to proceed to the next step. We were lucky to be granted a project in which we could buy an EWS (Engineering Workstation). The calculation ability was not so different, but the speed, tools and output quality of graphics were overwhelmingly improved. It did not take much time to implement the program onto the EWS (Hasegawa [12]). Photo 1 shows the perspective view of the ship with grids of coordinates and Photo 2 shows that of 2D wave. Photo 3 is the resultant view of the ship in wave,

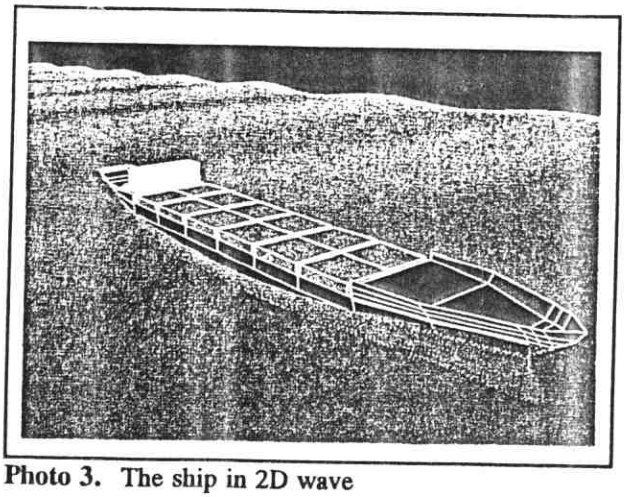

Photo 3. The ship in 2D wave

where hidden surfaces, half-transparency or ambient diffuse of lights are done by the hardware. Photos 4-7 show a series of motion up to the capsizing. At that time the computation of the ship motion was done separately with file output of the time history and the animation program read the movement from the file later. The automated VTR recording system is also developed, so each display output is captured into a video tape.

The system is quite effective to know the phenomena, the difference between calculation and experiment etc. As it is easy to set the camera point at any place such as shown in Photo 8 or even beneath the waterplane (Photo 9). Finally, it is also possible to set the camera in the bridge of the ship (Photo 10), though the camera didn't rotate. This suggests to us the possibility to develop a capsizing simulator.

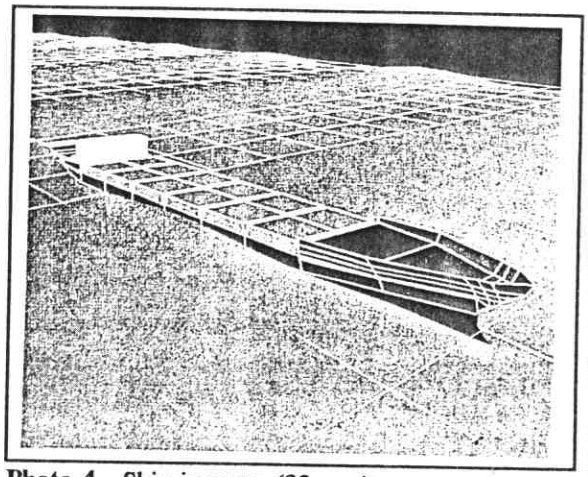

Photo 4. Ship in wave (23 sec.)

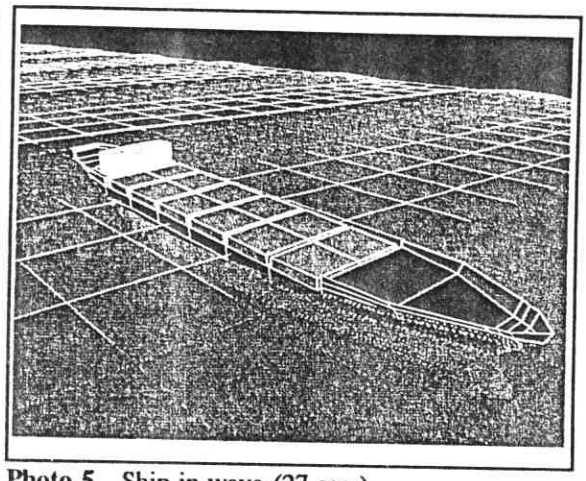

Photo 5. Ship in wave (27 sec.)

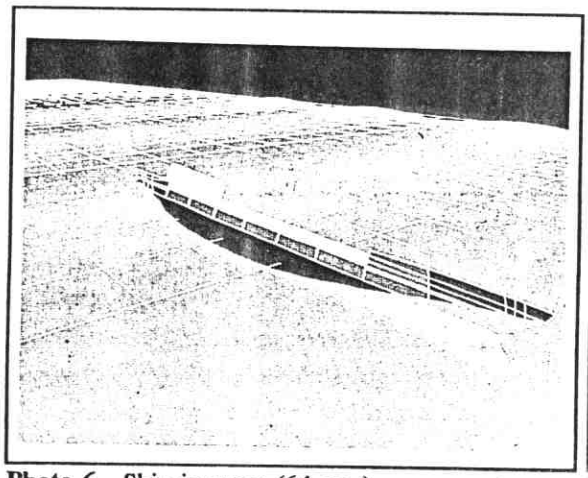

Photo 6. Ship in wave (64 sec.)

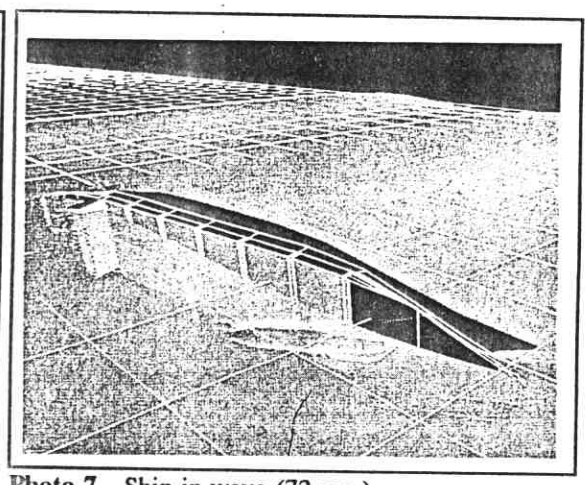

Photo 7. Ship in wave (72 sec.)

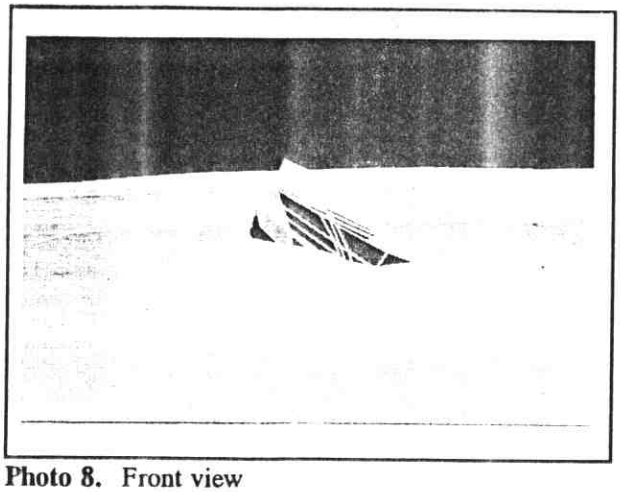

Photo 8. Front view

Through these experiences on theoretical and experimental approaches, and computer graphics, the prototype of a capsizing simulator was developed. The system graded up to the network distributed computation. A RISC-type high performance EWS calculates the motion every 1/4 second. The output is piped to another GWS (Graphics Workstation) through Ethernet, where graphic display is updated before the next calculation output reaches. The inputs of rudder and engine orders are supplied by a PC and transmitted to the EWS through RS-232C communication line. As the GWS has a real-time scan converter, the display output is projected onto a 100' screen. Though the hard copy of the screen is not so clear as to reproduce here, the movie video shall be shown at the presentation.

This kind of simulator will be useful for providing the guidance of operation in severe seas. Fig. 4 shows an example to demonstrate how this simulator will be used. There are several proposals on operational manuals in IMO (International Maritime Organization). Some are theoretical, some are experimental and the other are statistical ones. We can check the proposals using this simulator.

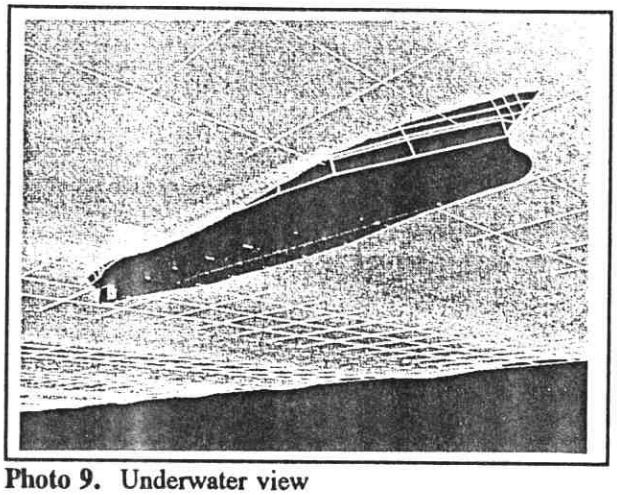

Photo 9. Underwater view

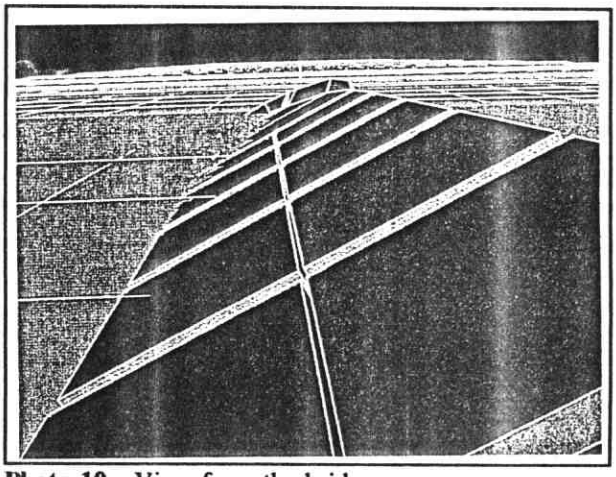

Photo 10. View from the bridge

CONCLUSION

As an example of the impact of new technology on marine industries, a prototype capsizing simulator is introduced. More attention should be paid to theoretical considerations on the equations of motion governing severe ship motion up to capsizing, confidence to build up a capsizing simulator is obtained.

Remaining works concerning the improvements on graphics and interfaces, may be easily done by commercial base, but new technology, especially software tools should be constantly monitored.

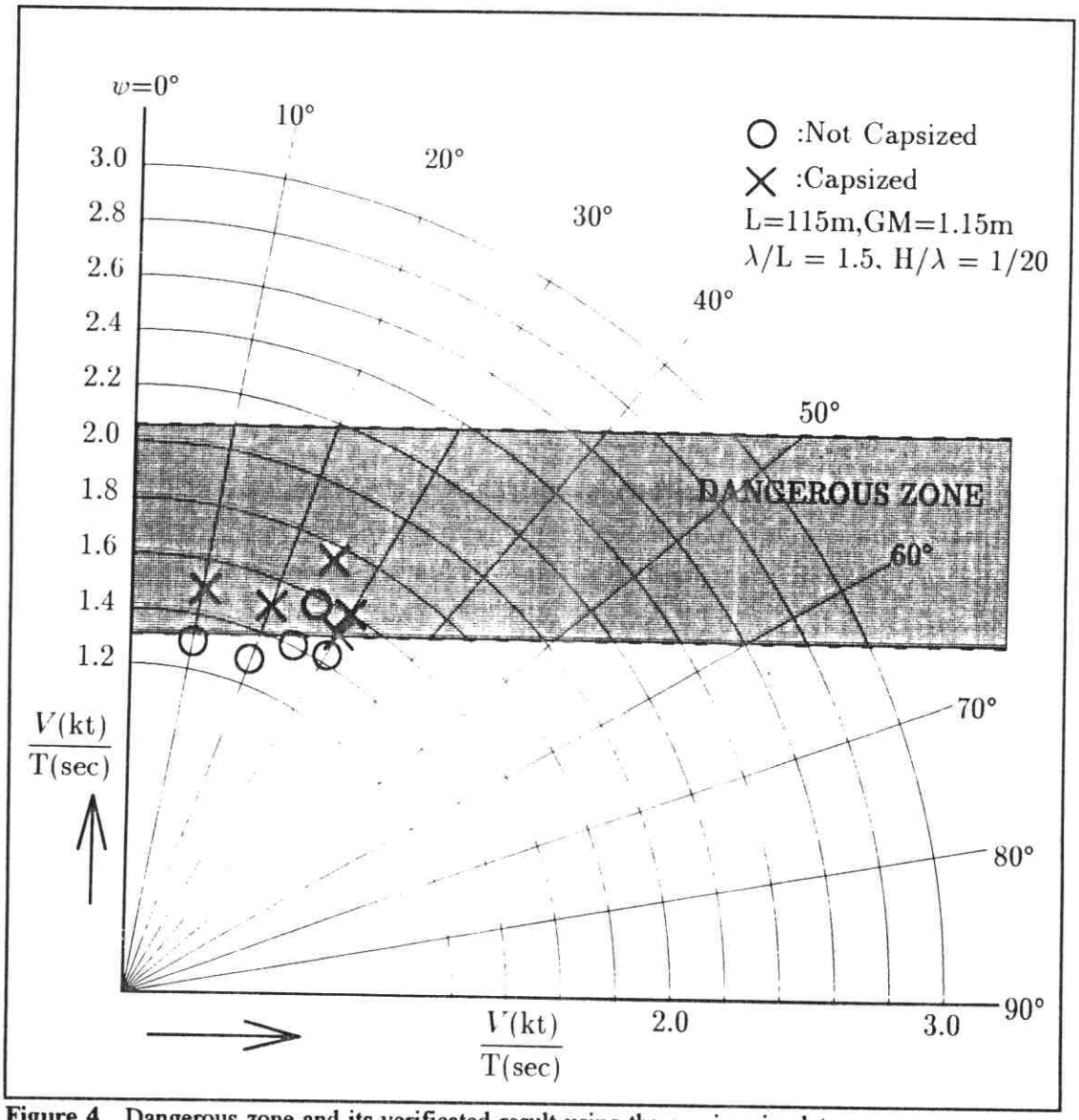

Figure 4. Dangerous zone and its verificated result using the capsize simulator

REFERENCES

1. Hamamoto, M. and Nomoto, K. *Transverse Stability of Ships in a Following Seas*, Proceedings of 2nd International Conference on Stability of Ships and Ocean Vehicles (STABILITY '82), Tokyo, 1982, p.137.

2. Hamamoto, M. *Transverse Stability of Ships in a Quartering Sea*, Proceedings of STABILITY '86, Vol.I, Gdansk, 1986, p.7.

3. Hamamoto, M. and Akiyoshi, T. *Study on Ship Motions and Capsizing in Following Seas* (1st Report - Equations of Motion for Numerical Simulation). J. of Society of Naval Architects of Japan (SNAJ), Vol.163, 1986, p.173.

4. Hamamoto, M. and Shirai, T. *Study on Ship Motions and Capsizing in Following Seas* (2nd Report - Simulation of capsizing). J. of SNAJ, Vol.165, 1989, p.123.

5. Hamamoto, M., Shirai, T. and Wakiyama, N. *An Analytical Approach to Capsizing of a Ship in Following Seas*. Proceedings of STABILITY '90, Napoli, 1990, p.354.

6. Hamamoto, M., Kim, Y.S. and Uwatoko, K. *Study on Ship Motions and Capsizing in Following Seas* (Final Report). J. of SNAJ, Vol.170, 1991, p.173.

7. Hamamoto, M. and Tshukasa, Y. *An Analysis of Side Force and Yaw Moment on a Ship in Quartering Waves* (in Japanese). J. of SNAJ, Vol.171, 1992, p.99.

8. Hamamoto, M., Kim Y.S. Matsuda, A. and Kotani, H. *An Analysis of a Ship Capsizing in Quartering Seas* (in Japanese). J. of SNAJ, Vol.172, 1992, p.135.

9. Hamamoto, M. and Kim Y.S. *A New Coordinate System and the Equations Describing Manoeuvring Motion of a Ship in Waves* (in Japanese). J. of SNAJ, Vol.173, 1993, p.209, or Hamamoto, M. Proceedings of the Workshop on Prediction of Ship Manoeuvrability, Fukuoka, Japan, 1992, p.61.

10. Hamamoto, M. and Saito, K. *Time-Domain Analysis of Ship Motions in Following Waves*. Proceedings of 11th Australasian Fluid Mechanics Conference, Hobart, Australia, 1992, p.355.

11. Hamamoto, M., Kim Y.S. and Matsuda, A. *Stability and Manoeuvrability of a Ship in Following Seas*. Proceedings of the Second Japan-Korea Joint Workshop on Ship and Marine Hydrodynamics, Osaka, Japan, 1993, p.131.

12. Hasegawa, K. *Computer Animation Visualizing Ship Capsizing* (in Japanese). PIXEL, No.87, 1989, p.73.

AUTHORS' BIOGRAPHIES

Kazuhiko Hasegawa

hase@naoe.eng.osaka-u.ac.jp

Associate Professor, Department of Naval Architecture and Ocean Engineering, Faculty of Engineering, Osaka University, e-mail:a62676a@center.osaka-u.ac.jp. He has been engaged in prediction and simulation of ship manoeuvrability, development of a ship handling simulator, automatic control of ship operation. He has also been engaged in ship design automation and his current interests lie on knowledge-based and fuzzy control ship navigation system and PC- and EWS-based simulators. Awarded Prize of the Society of Naval Architects of Japan, 1980 for his contribution on unusual phenomena in ship manoeuvrability, and Prize of the Kansai Society of Naval Architects, Japan, 1993 for his contribution of knowledge-based/intelligent control system for collision avoidance and berthing.

Masami Hamamoto

Professor, Department of Naval Architecture and Ocean Engineering, Faculty of Engineering, Osaka University. He has been engaged in hydrodynamics for ship manoeuvrability, theoretical and experimental analysis of capsizing in waves, and motion and control of hydrofoils. He is at the leading position of IMO regulation on capsizing in waves and manoeuvrability standard. Awarded Prize of the Society of Naval Architects of Japan, 1992 for his contribution on ship capsizing.

Hiroyuki Kotani

Matsushita Electric Company. He graduated from the Department of Naval Architecture and Ocean Engineering, Osaka University in 1991 (BSc) and got his Master degree in 1993 from the Graduate School, Osaka University. He has developed CG animation system of ship capsizing for his master thesis.

Notes for

PRELIMINARY STUDY TOWARDS A CAPSIZING SIMULATOR

Numerical and Physical Simulation of Ship Capsize in Heavy Seas, Glasgow. July 25, 1995.

AN EXPERIMENTAL STUDY ON FLOODING INTO THE CAR DECK OF A RORO FERRY THROUGH DAMAGED BOW DOOR

University of Osaka Prefecture
N. Shimizu, K. Roby and Y. Ikeda

1. Introduction

Shortly after midnight on sept. 28, 1994, the 15,566 ton, ferry ESTONIA sank in the stormy Baltic sea, during the overnight crossing from Tallin to Stockholm, causing the death of 852 of the 989 persons on board [1]. The sinking was caused by the tearing away of the 55 tons bow visor and the partly open inner door (loading ramp) through which the water flowed into the vehicle deck.

Few experimental and theoretical studies had been done on the survivability of damaged RORO ships in U.K.[2][3], Denmark[2] and Canada[4], for the damage in the midship region. So far, studies on the damage or loss of bow door was not done. The nature of water entering the ship through a bow opening and the phenomenon due to the presence and motion of water on deck are unknown. By our present studies, we are trying to understand these problems. We have done experiments with the model of a Car Ferry, with bow openings in calm sea and regular head waves at different advance speeds. The heave and pitch motions and the wave profiles were measured. From these experimental data, the amount of water on deck with respect to time, minimum amount of water on deck which will cause static capsize, the time required for the static capsize were found out. Further analysis of the experimental data is in progress.

2. Experiment

2. 1 Model

A 2 m long model of a 1500 GRT Car ferry of length 75 m, breadth 13.5 m, depth 8.5 m and draft 4.15 m was used for the experiment. The model breadth is 0.36 m, depth is 0.292 m and the height of cardeck from keel is 0.161 m. The depth of the cardeck is 0.131 m. The top of the car deck is covered by acrilic sheet. The bow of the model was cut open to represent the missing bow door. The experiments were done with two widths of openings of 0.099 m (Full) and 0.0495 m (Half). A bodyplan and a photograph of the model is shown in Fig.1.

2. 2 Experimental setup

The model was connected to a Motion Measuring Device which was fitted on the Towing carriage of a Towing Tank (70 m x 3 m x 1.6 m) in University of Osaka Prefecture. The connections allowed freedom only for the pitch and heave motions. These two motions and the wave profiles were measured using potentiometers and servo-needle wave probe, at definite intervals of time. Also the views of the bow opening and the decks were recorded using two video camerae. Fig.2. shows a view of the experimental setup.

2. 3 Experimental condition

The model was run at different Froude numbers with regular head waves of different λ/L (λ is wave length) and heights. To get the mean value of the heave motion data which means the time-variation of the sinkage of the ship, heave values were measured in calm condition for zero advance speed, before every run.

The ranges of values are as follows :

Froude number	: 0 - 0.3
λ/L	: 0.6 - 1.8
Wave height	: 0.04 - 0.10 (m)

Bow opening width - Full = 0.099 m ; Half = 0.0495 m

2. 4 Analysis and Results

Heave and pitch traces were plotted for each run. Some examples of them are shown in figures 3 to 6. Fig. 3 is for a case without any flooding of the car deck. Its heave and pitch motions are almost steady. Fig. 4 is for light flooding of the car deck. In this case, the mean heave changes with time due to the flooding of car deck, and the rate for the full opening case is much larger than that for the half opening case. Fig. 5 is for heavy flooding, at fast advanced speed. The model was rapidly drowned due to flooding for full opening case. Fig. 6 shows a case with non-linear motion. Analysis of these motion behaviour are being done. These examples of the experiments demonstrates that the characteristics of the ship motions significantly depend on the advance speed, the wave period, the wave height and the area of the bow opening.

Measured maximum depths of water on the car deck at the bow door are shown in Figs. 7a, 7b and 7c. These results are obtained from experimental data of the ship motions and that of the waves at the early stages (i.e., water on deck may not be large) and the whole duration of each run. In these figures, the calculated relative wave heights by Ordinary Strip Method are also shown, to be compared with the experimental results. In these calculations the flooded water on the car deck is not taken into account. The

measured water levels are more than the calculated values, in all the figures. In almost every case - included in the figures - there is flooding of the car deck, since the water height from car deck level is more than zero. The flooding is more for the full width bow opening case than for the half width bow opening case. The time at which the maximum values occur varies from the initial stages of the run to its final stages. As advance speed increase, the water height increase as shown in Figs. 7b and 7c. The difference between the measured and the calculated water height increases with advance speed because the calculation method does not take into account advance speed effect, except the frequency change due to speed.

Fig. 8 has some photographs taken during the experiments which show the extreme motion of the ship, sometimes immersing the whole bow opening.

The water on deck at definite time intervals can be calculated using the mean value of the heave motion. Some of the results are shown in figures 9 and 10. Fig. 9 shows the effect of Froude number and Fig. 10 shows the effect of λ/L. It can be seen that the water on deck increases with increase of Froude number, increase of wave height and wider bow opening. For the same wave height and Froude number, the maximum amount of water on deck is for λ/L=1.0.

The GZ curves (including the effect of deck water) and the static equilibrium angles of heel for the experimental ship were found for different amounts of water on deck. The values are given in Table 1. Fig. 11 shows that the loss of righting lever due to the effect of deck water is very high. It can be seen in Fig. 12 that the ship capsizes due to the effect of deck water, whereas the ship is very stable for a fixed weight of the same amount as the free water on deck. Fig.13 shows the effect of deck water on the equilibrium angle of heel. The minimium amount of water on car deck for the static capsize is 1040 m^3 for the ship and 0.0197 m^3 for the model, which is shown in Figs. 9 and 10 as a capsize limit. The time for the accumulation of this much water on the deck of the model is taken as the capsizing time. Capsizing time and the number of waves encountered before capsize are given in Table 2. At Fn=0.3 and λ/L=1.8, the ship capsizes within just 4 waves.

The obtained values of the water on deck in the present experiments are for a model which is prevented from heeling, or no rolling motion. In the real case, the model or ship will heel due to the movement of water on deck, which will change the area of bow opening exposed to water and the entry of water into the car deck. This may speed up the capsizing act. This may suggest that an experiment of a ship in three degrees of freedom, heave, pitch and roll, should be carried out.

It can be seen that the water that cause the capsizing occupies only a small portion

of the total volume of the car deck. The unrestricted flow of water into the full length cardeck will surely cause capsizing. However, the rate of flow of water into the ship can be reduced by reducing the speed or stopping the ship. This may suggest that the navigation of a damaged RORO ship is very important to survive.

3. Conclusion

The experimental study was conducted on the model of a car ferry with openings on the bow, in regular head seas. The amount of water accumulated on the deck, found from the data, shows that at higher speeds and higher wave heights, the ship will capsize. Reducing the speed in the case of bow damage may help in avoiding or delaying capsize. It should be noted that in severe motion conditions at very high advanced speed the ship may capsize within just 4 waves.

REFERENCE

[1] 'Part-Report, covering Technical issues, by the Joint Accident Investigation Commission of Estonia, Finland and Sweden on the capsizing of MV ESTONIA'. April, 1995.

[2] Marine Safety Agency, U.K. : 'Reports on Research into Enhancing the Stability and Survivability Stands of RO-RO Passenger Ferries'.

[3] Vassalos D. and Turan O. : 'The Influence of Design Constraints on the Damage Survivability of RO-RO vessels'.

[4] John T. Stubbs, et al : 'TP 12310E Flooding Protection of RO-RO Ferries, Phase I (Vol.1)'. Transports Canada.

Scale 1 : 37.5 Depth of ship = 10.95 m
Height of cardeck above keel = 6.038 m
Depth (inside) of cardeck = 4.912 m

(m^3) Volumes	*	(m) KG	*	(deg) Equili.
Ship (4.15m)	* DeckW (depth) (of water, m)	*Total	*Ship	*Combined* Angle
2350.6	49.4(0.049)	2400.0	5.6	5.60947 4.68
2350.6	98.8(0.098)	2449.4	5.6	5.61956 8.72
2350.6	148.2(0.147)	2498.8	5.6	5.63022 12.70
2350.6	197.6(0.197)	2548.2	5.6	5.64144 16.76
2350.6	247.1(0.246)	2597.6	5.6	5.65316 20.59
2350.6	296.5(0.295)	2647.1	5.6	5.66538 24.38
2350.6	346.0(0.344)	2696.5	5.6	5.67805 27.91
2350.6	395.4(0.393)	2746.0	5.6	5.69115 31.04
2350.6	444.9(0.441)	2795.4	5.6	5.70467 34.09
2350.6	496.9(0.494)	2847.5	5.6	5.71931 36.94
2350.6	598.8(0.595)	2949.4	5.6	5.74913 41.55
2350.6	700.7(0.696)	3051.3	5.6	5.78035 45.90
2350.6	802.6(0.797)	3153.2	5.6	5.81281 49.64
2350.6	904.5(0.898)	3255.1	5.6	5.84641 55.77
2350.6	1006.4(0.999)	3357.0	5.6	5.88103 66.38
2350.6	1108.3(1.100)	3458.9	5.6	5.91654 NO
2350.6	1210.2(1.201)	3560.8	5.6	5.95292 NO
2350.6	1312.1(1.302)	3662.7	5.6	5.99008 NO

Max. volumes (m^3) and [KB(m)]:
Ship = 9129.7 [6.256] CarDeck = 4968.8 [8.497]
Under CarDeck = 4158.7 [3.579]

Table 1: Static effect of Water on Deck (ship)

Min. volume of water on car deck for capsize = 0.0197 m^3
(for model) Model length = 2 m

Capsize time in Sec.(Number of Waves encountered)

	λ/L	0.6		1.0		1.8	
	Wave	opening width					
Fr.No.	Height	Full	Half	Full	Half	Full	Half
0.1	4 cm	-	-	-	-	-	-
	8 cm	-	-	-	-	-	-
	10 cm	-	-	15(16.6)	-	-	-
0.2	4 cm	-	-	X	X	X	X
	8 cm	-	-	9(11.9)	-	-	-
	10 cm	9(16.8)	-	7(9.3)	-	-	-
0.3	4 cm	-	-	-	-	18	-
	8 cm	9(20)	-	3.5(5.4)	12.5(19.4)	3.5(3.6)	X
	10 cm	X	X	X	X	X	X

Full = opening width of 0.099 m X : no data available
Half= opening width of 0.0495 m - : no capsize with in 20 sec.

Table 2: Static Capsize time and Waves encountered

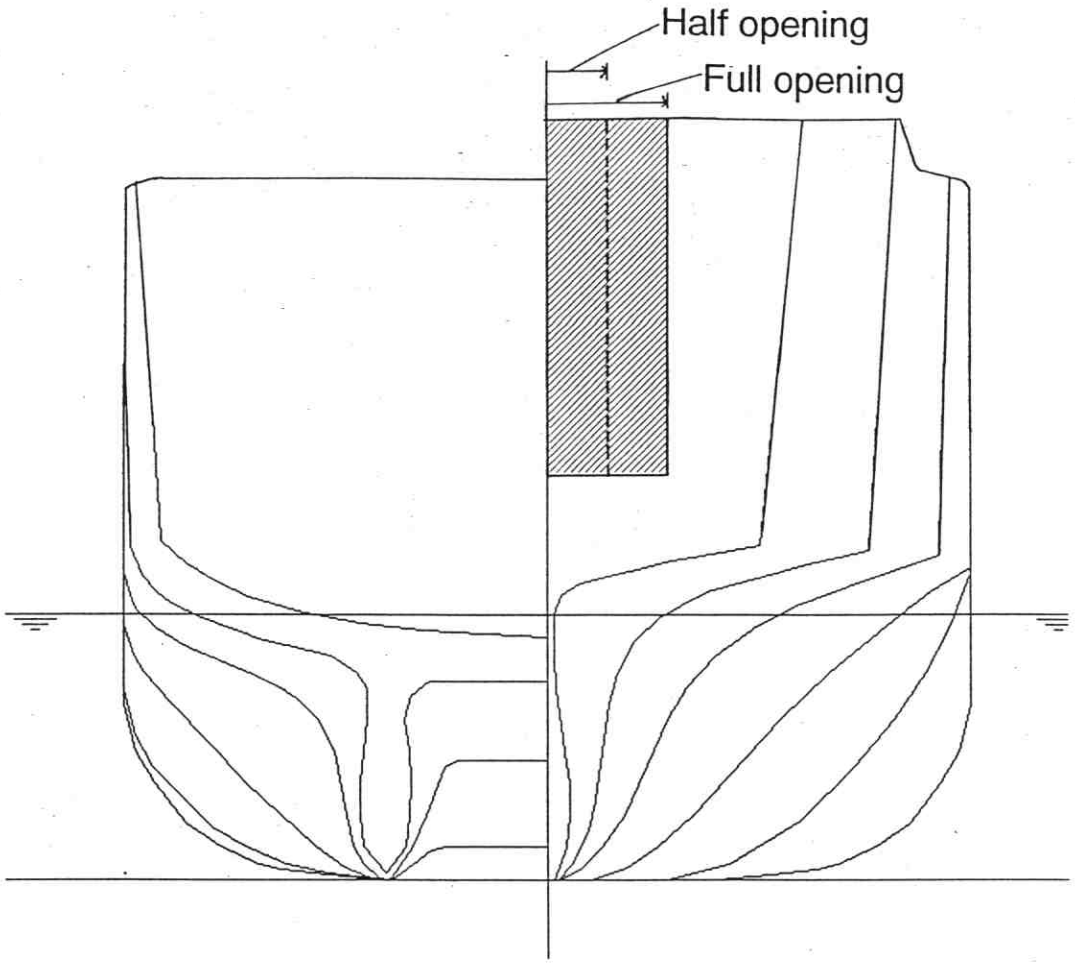

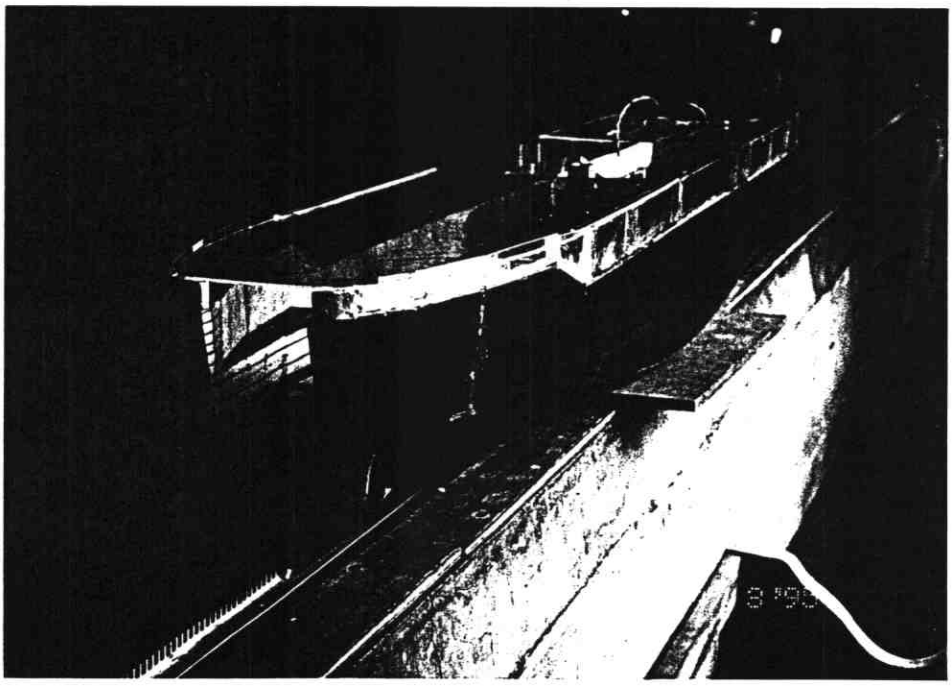

Fig. 1 Bodyplan and photograph of model

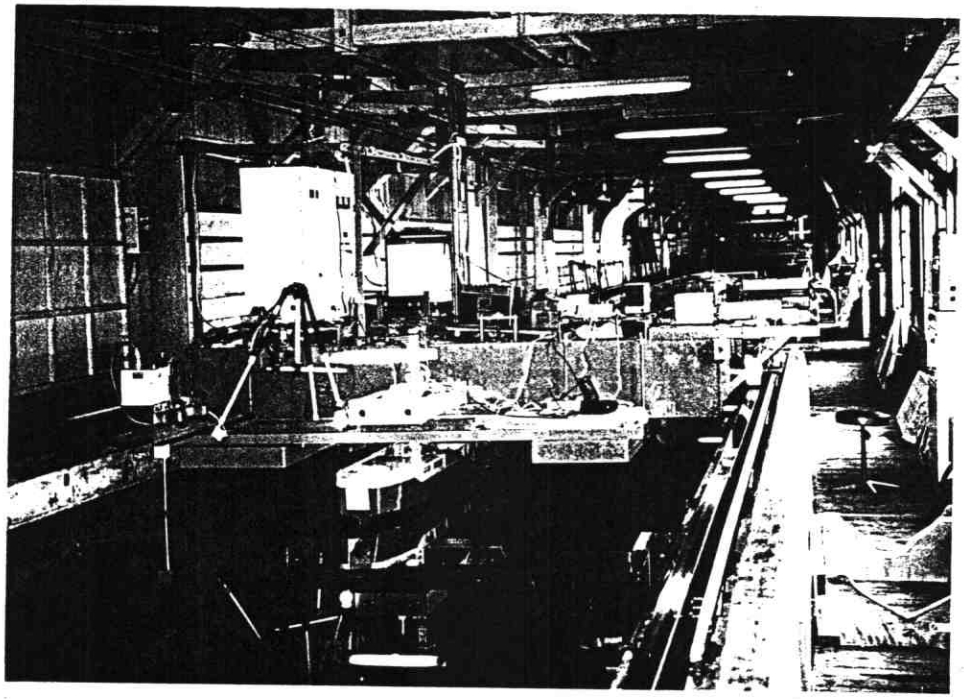

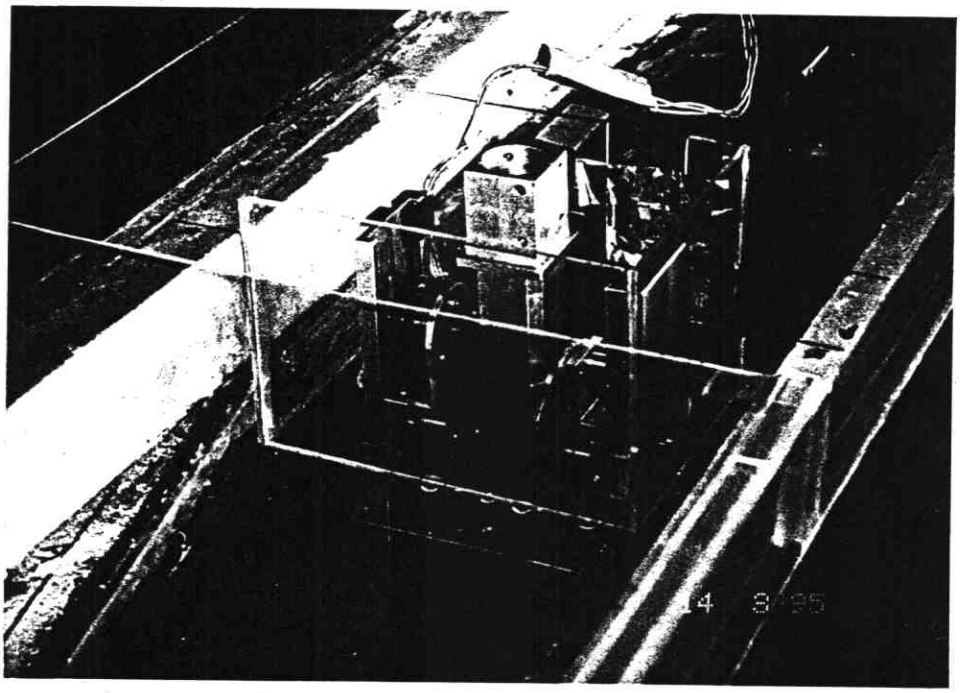

Fig. 2 Experimental setup

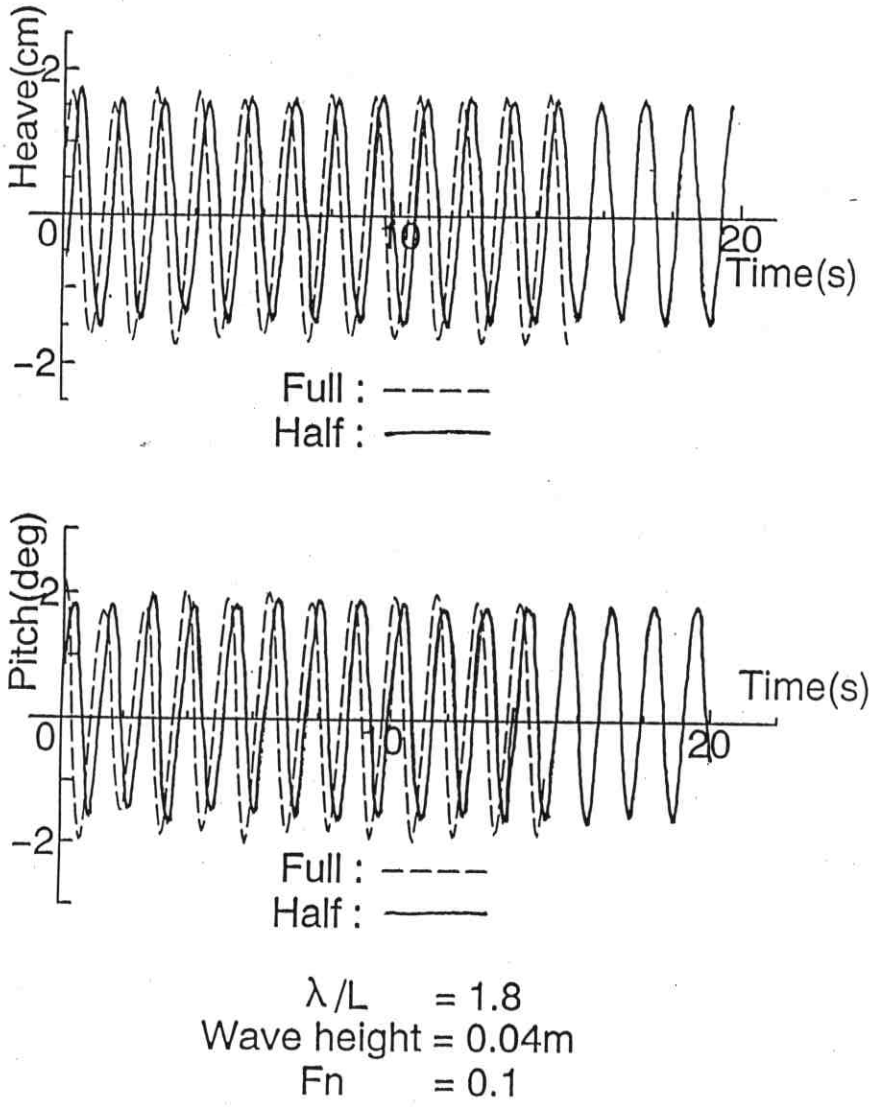

Fig. 3 Bow damage – no flooding occurs

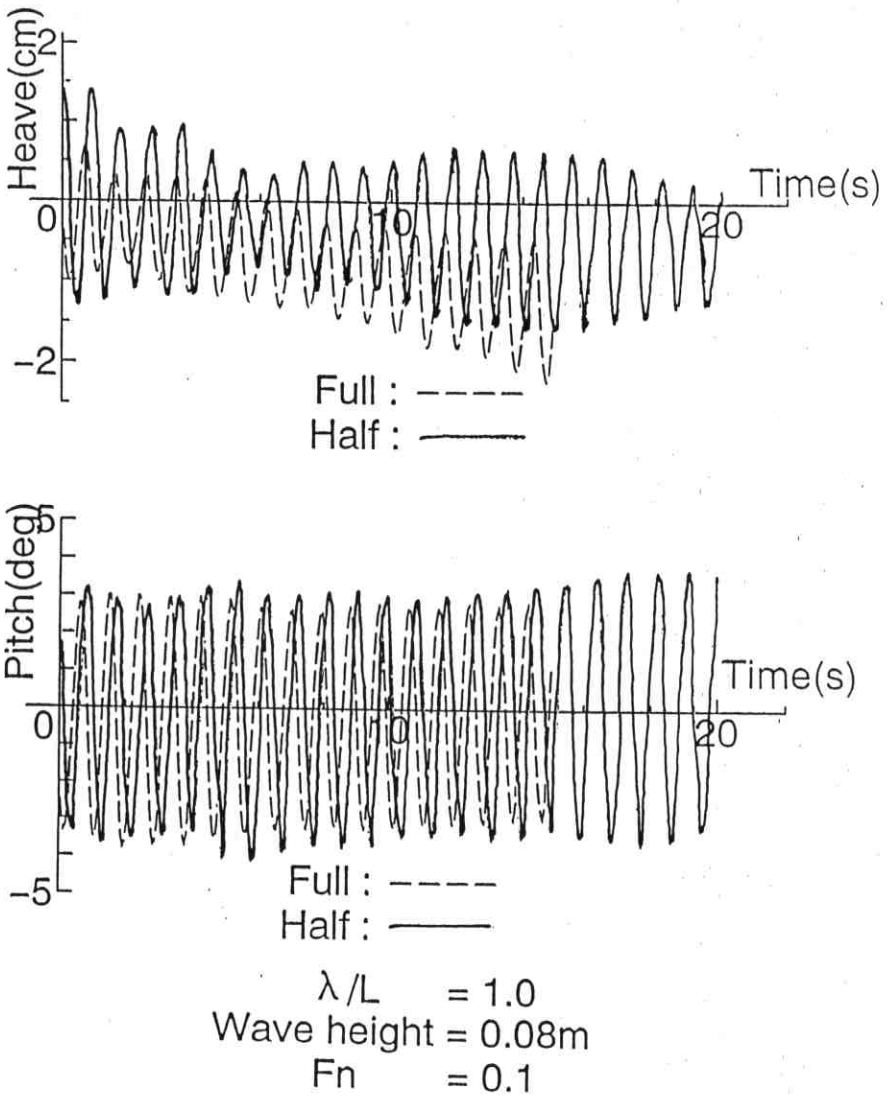

Fig. 4 Bow damage – light flooding occurs

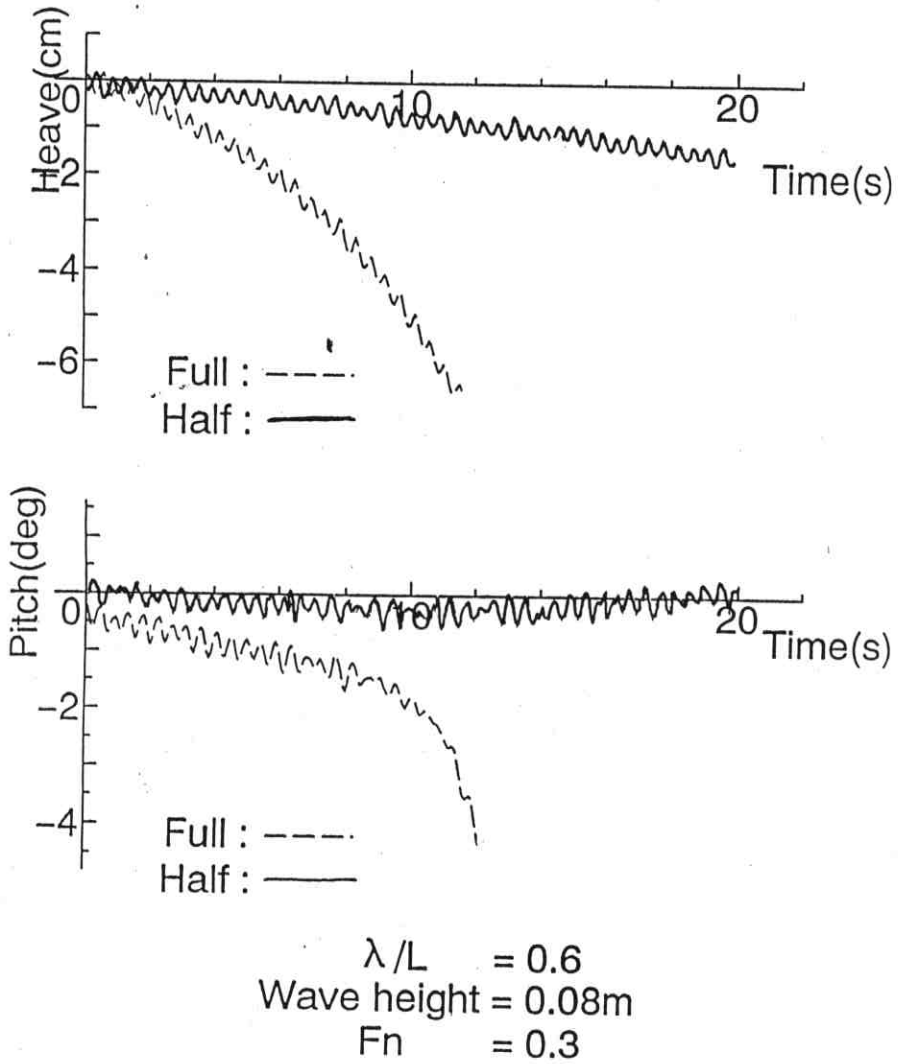

λ/L = 0.6
Wave height = 0.08m
Fn = 0.3

Fig. 5 Bow damage – heavy flooding occurs

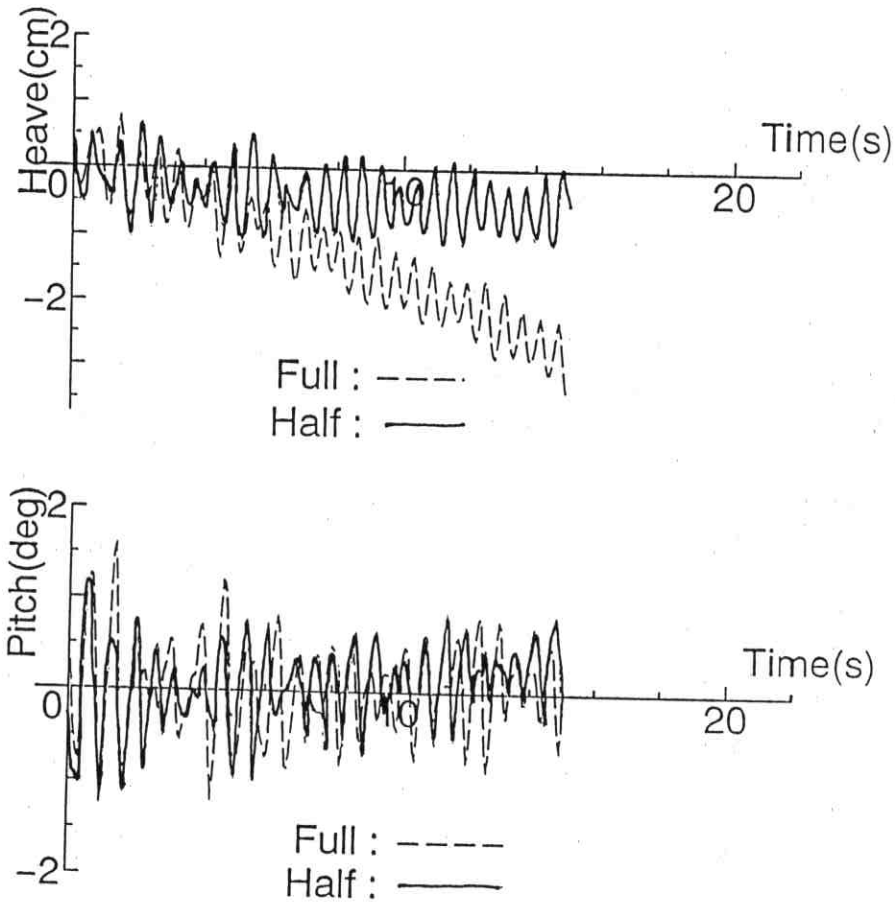

λ/L = 0.6
Wave height = 0.10m
Fn = 0.2

Fig. 6 Bow damage – non-linear motions can be seen

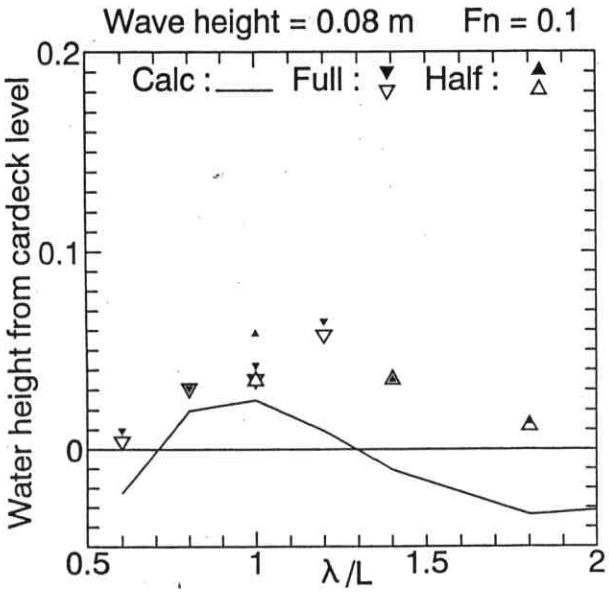

Fig.7a Water level at bow door (RORO ship)

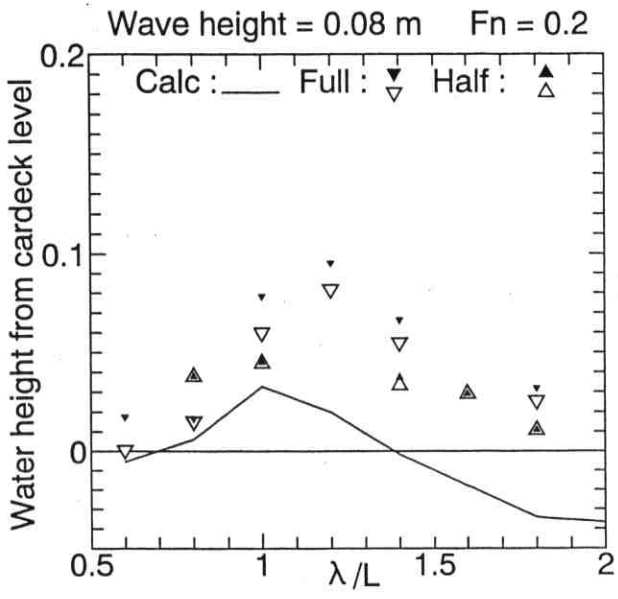

Fig.7b Water level at bow door (RORO ship)

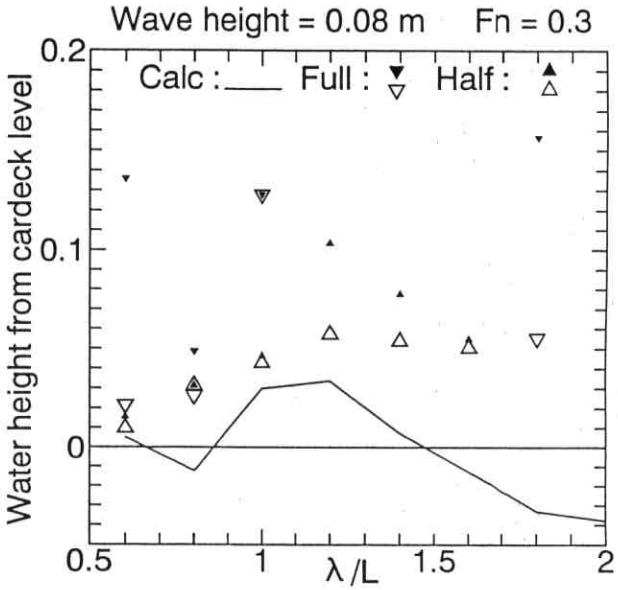

Fig.7c Water level at bow door (RORO ship)

▲▼ - max. during the whole run.

△▽ - max. within the first 3 seconds of the run.

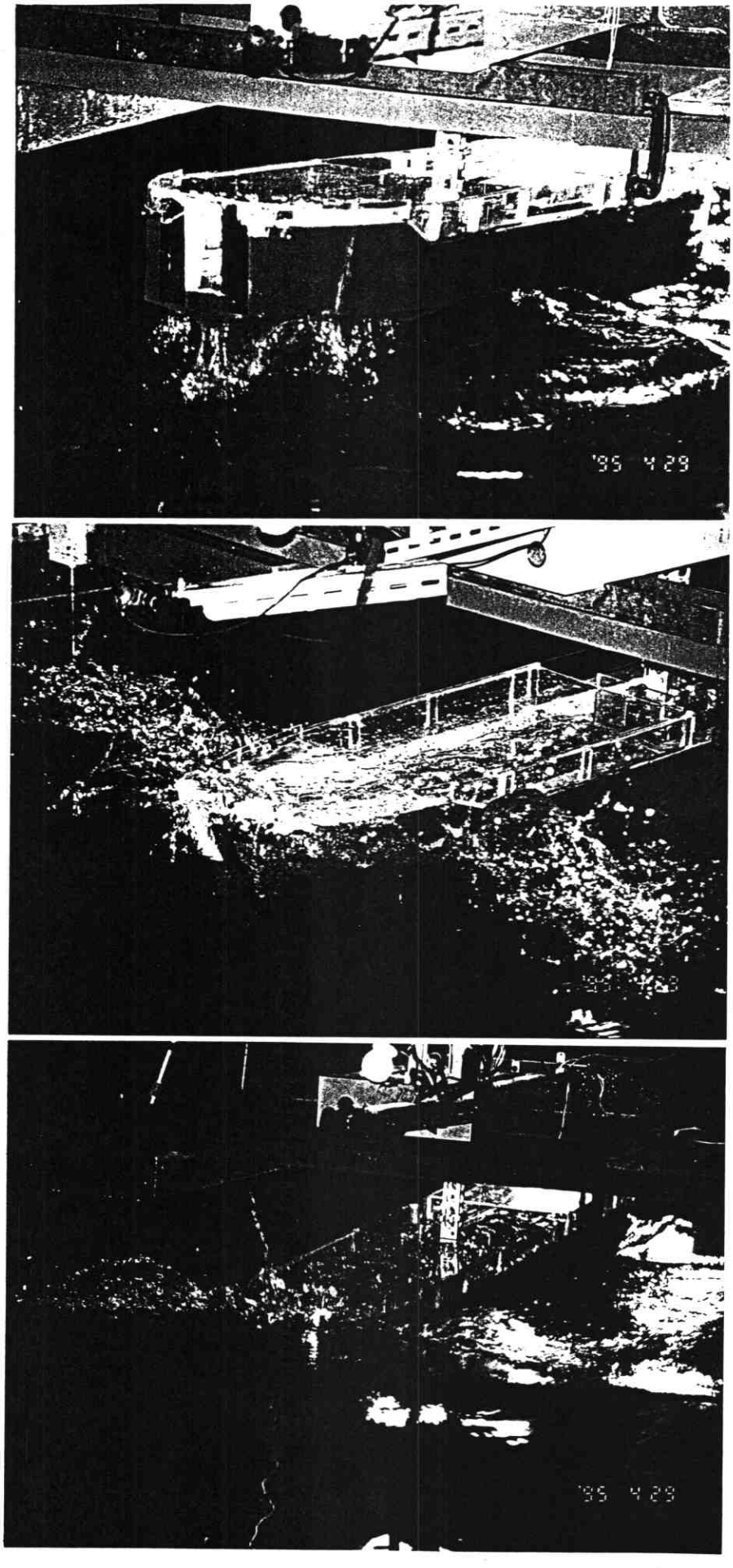

Fig.8 Photographs during Experiment

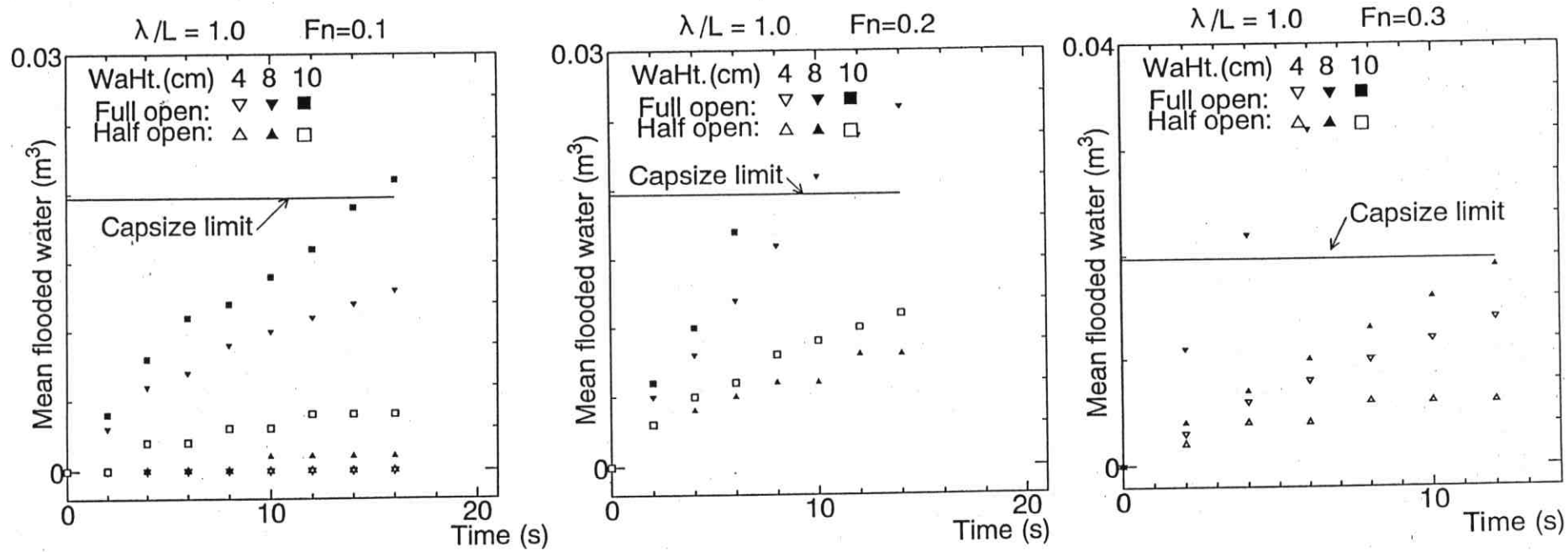

Fig. 9 Water on deck – Effect of Froude number

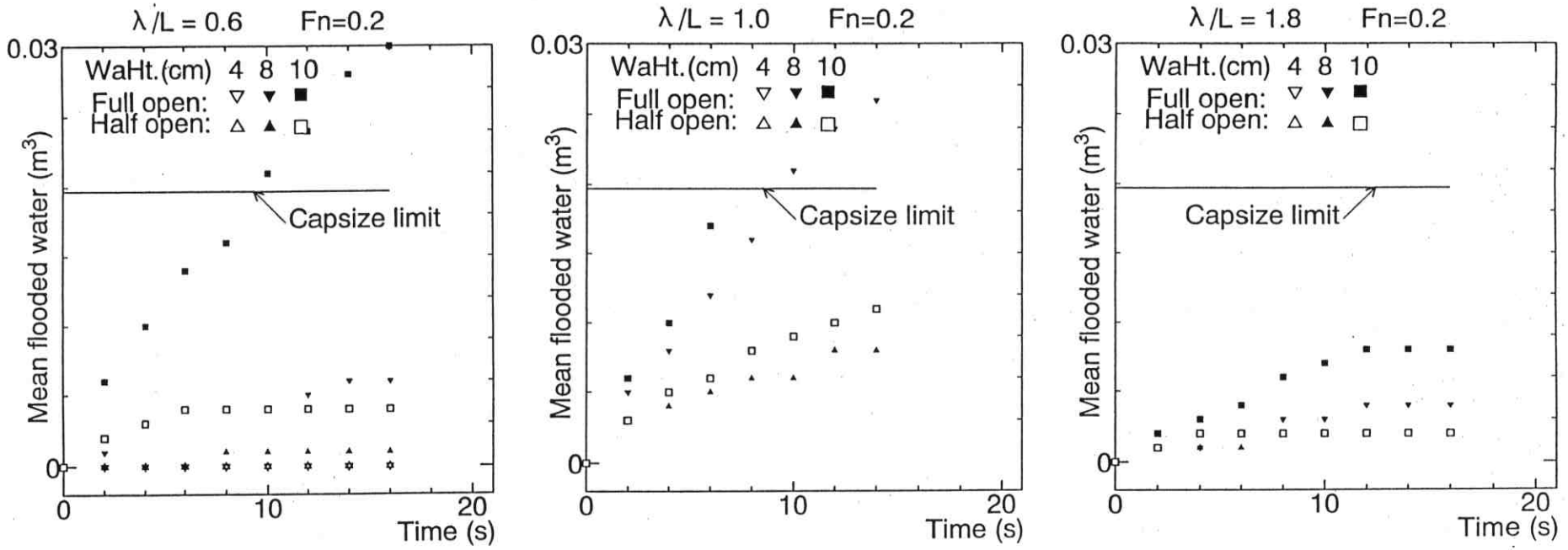

Fig. 10 Water on deck – Effect of λ/L

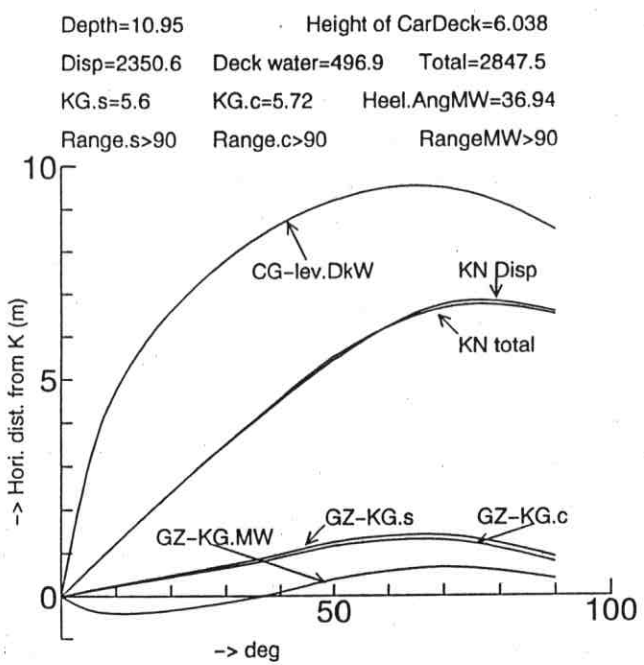

Fig. 11 Loss of Righting Lever due to water on deck

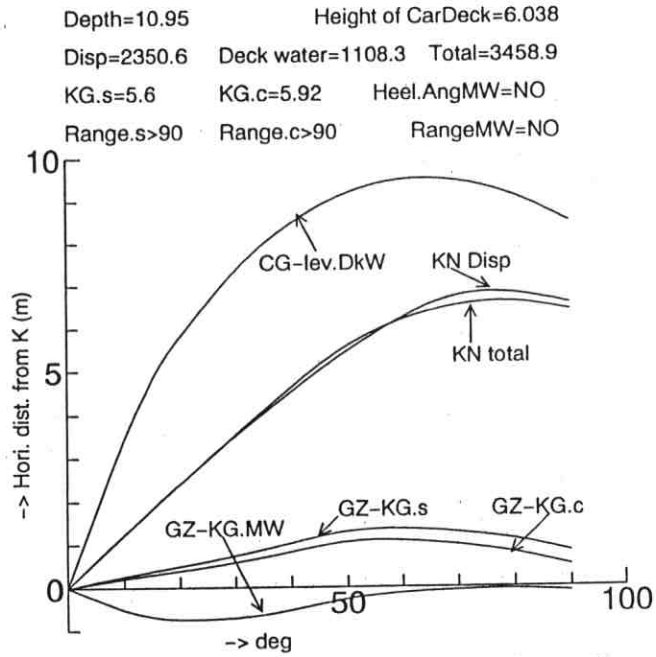

Fig. 12 Capsize due to the effect of Water on deck

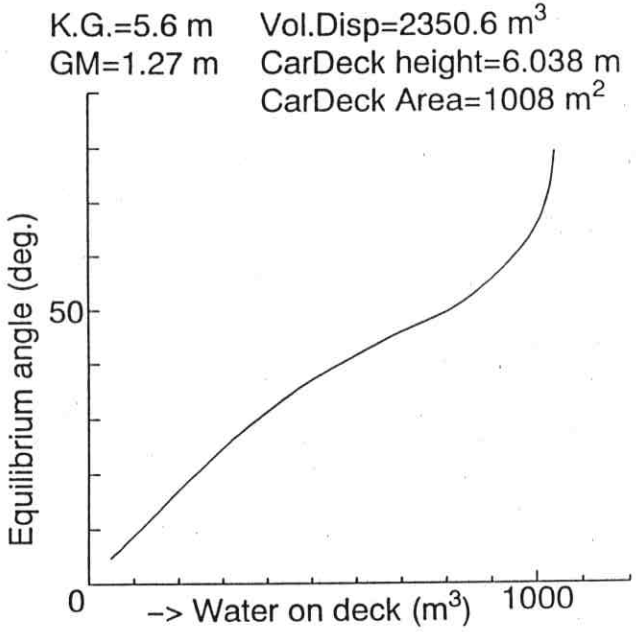

Fig. 13 Water on deck & Equilibrium angle